

Revised Paper – Text only rev2.doc

Date: 24th March, 2017

Title: Thermo-mechanically loaded GFRP single-bolt single-lap joints

Authors: *Geoffrey John Turvey, BSc, MSc, DIC, PhD, CEng, FICE, MIStructE, **M. Szulik, MEng

Affiliations: *Senior Lecturer, Department of Engineering, Lancaster University
** Research Student, Department of Electronic Warfare, Cranfield University

Corresponding author's contact details:-

Address: Engineering Department, Lancaster University, Gillow Avenue, Bailrigg, Lancaster, LA1 4YW, UK

Tel.: +44 (0) 1524 593088

Email: g.turvey@lancaster.ac.uk

Number of words in main text: 5417

Abstract

The paper describes 120 uniaxial tensile failure tests on pultruded glass fibre reinforced polymer (GFRP) single-bolt single-lap joints. For each joint the lap width to bolt/hole diameter ratio W/D and bolt diameter D were 4 and 10 mm, respectively. Five end distance to bolt/hole diameter ratios E/D and four test temperatures were investigated. The joints were sub-divided into 20 groups – one for each E/D and temperature combination - and each group comprised six nominally identical joints. In addition to the joint tests, a number of uniaxial tensile failure tests were carried out on the *virgin* GFRP plate of the joints' laps. Mean ultimate loads and extensions derived from the joint failure tests are presented and used to compile graphs of ultimate stress and overall failure strain as functions of joint geometry and test temperature, from which corresponding characteristic values have been obtained. In addition, *knock-down* factors, which express the ultimate stresses of the joints, relative to the ultimate stress of the *virgin* GFRP plate, have been derived. The knock-down factors have been compared with those obtained earlier for single-bolt double-lap joints. The factors may be useful for the preliminary design of single-bolt tension joints.

Keywords: Composite structures; Strength & testing of materials; Thermal effects

List of Notations

k constant (depends on the number of nominally identical values of the design quantity determined by testing)

σ_c characteristic value of the design quantity

σ_m mean value of the design quantity

σ_{sd} standard deviation of the design quantity

1. Introduction

Pultruded glass fibre reinforced polymer (GFRP) composite structural profiles, e.g. I-sections, channels, angles and flat plate, are being considered and used with ever increasing frequency for fabricated load-resisting structures (guard-rails, trusses, storage platforms, electricity pylons, footbridges etc.), because of their advantageous properties (low self-weight, excellent corrosion, thermal and electrical resistance, low life-time maintenance costs etc.). Load transfer between the profiles of these structures is commonly effected by mechanically fastened joints. Because pultruded GFRP is an orthotropic elastic – brittle material, load transfer in, and failure of GFRP joints differs from that in metallic joints. This situation has been the catalyst for significant ongoing research on the behaviour of bolted tension (plate-to-plate) and bolted flexural (beam-to-column) joints. The focus of the present investigation is on the single-lap type of the former joints, which, for example, arise in lateral bracing of beams and sway bracing of frames. In the succeeding paragraphs, research on pultruded GFRP tension joints is very briefly reviewed to provide the background and justification for the present investigation.

During the 1990s several noteworthy experimental investigations were reported on pultruded GFRP single- and multi-bolt double-lap (plate-to-plate) joints subjected to uniaxial tension (Abd-El-Naby and Holloway, 1993a & 1993b; Cooper and Turvey, 1995; Rosner and Rizkalla, 1995; Turvey and Cooper, 1995; Hassan, Mohamedien and Rizkalla, 1997). The GFRP material used in these tests was cut out of the webs and flanges of wide flange (WF) sections and flat plate, the thicknesses of which varied from 6.4 mm to 19.1 mm. Moreover,

1 all of the tests were carried out with the tension axis parallel to the pultrusion direction, so that both were
2 aligned with the glass fibre roving reinforcement. Somewhat later, an investigation into the effects of off-axis
3 tensile loading on the failure behaviour of single-bolt double-lap joints in 6.4 mm thick plate was reported
4 (Turvey, 1998). The results of these investigations, together with those of several others not cited, constitute a
5 large database of ultimate tensile stresses of single- and multi-bolt double-lap joints. However, it should be
6 appreciated the test data are only valid for ambient temperature conditions (circa 20 °C). Furthermore, it should
7 be recognised that such joints in the types of structural application mentioned above may experience
8 temperatures much greater than 20°C. In some middle-eastern countries structures, and therefore joints, may
9 experience temperatures up to 50+°C for part of the day at certain times of the year.

10 In a more recent investigation (Turvey and Wang, 2007a), the effects of hot-wet conditioning on the failure
11 response of single-bolt double-lap tension joints was investigated for four joint geometries, each corresponding
12 to one of the basic failure modes (bearing, cleavage, shear and tension) observed at ambient temperature. A
13 Taguchi analysis of the test data was also carried out (Turvey and Wang, 2009), which revealed that temperature
14 was the major degrading influence on the joints' load capacities. More comprehensive test data on the effects of
15 thermal conditioning on the failure of single-bolt double-lap tension joints in pultruded GFRP plate has been
16 reported recently (Turvey and Sana, 2016).

17
18 In contrast to the relative abundance of test data/design guidance on the ultimate tensile loads of pultruded
19 GFRP bolted double-lap joints, such information for single-bolt single-lap joints is limited, though data from 45
20 tensile tests on single-bolt single-lap joints with the bolts torqued to 3 Nm has been reported (Turvey, 2012).
21 The data showed how the mean ultimate loads/stresses and failure modes varied with joint geometry, i.e. lap
22 width to hole/bolt diameter ratio W/D and end distance to hole/bolt diameter ratio E/D. In a follow up
23 investigation (Turvey, 2013) the results of a series of single-bolt single-lap tension joint tests, in which higher
24 torques were used to tighten the bolts, revealed that the joints' ultimate loads/stresses did not increase in direct
25 proportion to the increase in bolt torque. One of the first investigations of the tensile failure of two-bolt single-
26 lap joints in pultruded GFRP plate with the bolts on the tension axis was also reported recently (Turvey, 2014).
27 The investigation highlighted the effect of bolt pitch distance to hole/bolt diameter ratio P/D on the joints'
28 ultimate loads/stresses. It was shown that increasing the P/D ratio from 3 to 4 did not increase the ultimate
29 load/stress significantly. Nevertheless, the ultimate loads/stresses of the two-bolt single-lap tension joints were
30 substantially higher than the single-bolt single-lap joints with the same W/D and E/D ratios. All of the
31 aforementioned tensile failure tests on single-bolt single-lap joints were carried out at ambient temperature
32 (circa 20°C).

33
34 It appears that the effects of elevated temperature on the failure behaviour of single-bolt single-lap tension joints
35 in pultruded GFRP plate have yet to be reported. Recognition of this situation was the stimulus for the present
36 investigation, the results of which are relevant to the preliminary design of such bolted joints at the ends of
37 lateral and sway bracing members.

38
39 Details of tensile tests carried out on the GFRP plate to quantify its mean ultimate load/stress are presented first.
40 This is followed by descriptions of the single-bolt single-lap joint geometries and the joint test matrix. Brief
41 details of the joint fabrication and test procedures, together with comments on test data acquisition, then follow.
42 Thereafter, the mean ultimate loads and overall extensions obtained from the joint tests are tabulated. This data
43 is used to present graphs of the joints' mean ultimate stresses and strains as functions of joint geometry and test
44 temperature. In addition, tabulated values of characteristic ultimate stresses and strains are presented. Knock-
45 down factors are also derived for mean and characteristic ultimate stresses and compared with corresponding
46 factors for single-bolt double-lap tension joints. Finally, the main observations/conclusions of the investigation
47 are summarised.

48 49 **2. Mechanical properties of pultruded GFRP plate**

50
51 The pultruded GFRP composite material used to fabricate the single-bolt single-lap joints was EXTREN® 500
52 and 525 series 6.4 mm thick flat plate. The 525 series plate was used mainly for the joints tested at the highest
53 temperature, because of a shortage of 500 series plate. The weight percentage of glass fibre reinforcement is the
54 same in both plate series and is in two forms, namely rovings (unidirectional parallel fibre bundles) and
55 continuous filament mat (CFM). The rovings determine the plates' longitudinal stiffness and ultimate stress,
56 whereas the CFM determines these properties in the transverse direction. Consequently, the plate is orthotropic
57 with its principal axes parallel and normal to the pultrusion direction. The plate's fibre reinforcements are
58 encapsulated and rigidised by an isophthalic polyester resin. The weight percentages of fibre and resin are
59

typically about 30% and 70%, respectively with the latter percentage including up to 10% of calcium carbonate or kaolin filler. The 525 series plate incorporates a surface fire retardant and a UV inhibitor.

A series of tension coupon tests were carried out to determine the 500 and 525 series plates' tensile mechanical properties. Six 300 mm long nominally identical rectangular coupons were cut out of the 500 series plate with their longer sides parallel to the rovings. These untabbed coupons were loaded to failure in tension in a manually controlled Amsler hydraulic test machine. Details of their mean cross-section dimensions and individual ultimate loads/stresses, as well as their corresponding mean values are given in Table 1. A further five nominally identical tension coupons were cut out of the 500 series plate. Back-to-back uniaxial strain gauges (120 ohm internal resistance and 10 mm gauge length) were bonded to the centre of each coupon with their sensitive axes oriented along the coupon's longitudinal centre line. These coupons were tested in the Amsler machine to determine the plate's mean longitudinal elastic modulus. The loads were applied in 1 kN increments up to 12 kN prior to unloading in 1 kN decrements and strains were recorded for each increment/decrement. Details of the coupons' geometry, their individual elastic moduli and mean modulus are presented in Table 2(a).

Four wider tension coupons, with the same length as the 500 series coupons, were cut out of the 525 series plate, so that their longitudinal elastic moduli and ultimate strengths could be determined. The coupons were tested in an Instron 8802 servo-hydraulically controlled testing machine under displacement control at a rate of 2 mm/minute. The coupon geometries, individual moduli and mean elastic modulus are given in Table 2(b).

Based on the ultimate load/stress data presented in Tables 1, 2(a) and 2(b) and other data (Turvey and Sana, 2016), it is concluded that the tensile properties of the 500 and 525 series pultruded plate are similar. This conclusion is also confirmed by the same minimum property values for the 500 and 525 series plate given in the manufacturer's design manual (see the Strongwell website).

3. Single-bolt single-lap joint geometry and joint test matrix

A sketch of a single-bolt single-lap tension joint is shown in Figure 1(a). The thickness of the GFRP packing bonded to the unbolted ends of the GFRP laps is equal to the thickness of the laps, i.e. nominally 6.4 mm. Their primary purpose is to ensure that the joints' laps do not bend when the packing and ends of the laps are clamped by the test machine's grips prior to loading in tension. Figure 1(b) shows a joint ready for testing in tension (at circa 20°C) in the Instron machine; clearly the GFRP packing is effective in suppressing lap-flexure prior to loading.

The geometry of the single-bolt single-lap tension joint is defined in terms of the geometry of its laps, as shown in Figure 2. The grip length GL is equal to the length of the GFRP packing. The lap length L is defined by the distance from the centre of the bolt hole to the inner edge of the packing. W is the lap width, E is the distance from the free end of the lap to the centre of the bolt hole and D is the diameter of the hole. All lap dimensions, except the end distance E, are constant, i.e. GL, L and W are 50, 100 and 40 mm, respectively. The end distance E varies from 20 to 50 mm. The geometry of the joint is defined by combining the three geometric parameters, D, E and W, into the width to hole diameter ratio W/D and the end distance to hole diameter ratio E/D. Furthermore, the bolt and hole diameters are equal, hence the bolt - hole clearance is zero.

The foregoing geometric ratios, together with the test temperatures and the number of nominally identical joints in each parameter group, define the extent of the present investigation of single-bolt single-lap tension joints. Furthermore, as it was intended that the joint test data should complement recently reported single-bolt double-lap tension joint test data (Turvey and Sana, 2016), the joints used 10 mm diameter stainless steel bolts. In addition, they all had the same W/D ratio and E/D ratios, the latter spanning the practical range of values. The joints were also tested at the same four temperatures (20, 40, 60 and 80°C), the highest being 15 °C above the material's recommended maximum operating temperature (according to the Strongwell design manual). Thus, the bolt/hole diameter together with the W/D, E/D ratios and the test temperatures define the joints' test matrix given in Table 3.

4. Brief remarks on joint fabrication

The laps of the joints were fabricated by cutting 40 mm wide rectangular strips out of the pultruded GFRP board with their longer sides parallel to the rovings, The lengths of the strips were equal to $2(E+2GL+L)$. Their widths and thicknesses were then measured at three locations along the length, i.e. near the centre and the two ends, to determine the joints' mean thicknesses and widths. The strips were then cut transversely to provide two laps and two packings. An indelible ink pen was used to mark the position of the centre of the bolt hole and the interior

1 edge of the packing on each lap and to provide a label identifying the joint number, its test temperature and its
2 E/D and W/D ratios. Each lap, in turn, was clamped to a timber base on the platen of a pillar drill. The purpose
3 of the timber was to minimise break-through delamination during hole-drilling. The tungsten carbide tipped drill
4 was then positioned over the hole-centre mark and the 10 mm diameter bolt hole was drilled through the lap.
5 The drill's rotational speed was 900 rpm. After completing the drilling operation, one face of the packing was
6 abraded to remove its surface veil. Likewise, on one lap face the area between interior edge of the packing and
7 the end of the lap was abraded to remove its surface veil. Araldite epoxy adhesive was then applied to the
8 abraded faces of the packing and the lap. Four 5 mm lengths of 1 mm diameter wire were placed in the adhesive
9 on the lap to ensure a uniform bond-line. The packing was then placed on the adhesive on the end of the lap and
10 carefully adjusted before both were clamped together. Excess adhesive was removed and the lap and packing
11 were left for 24 hours to allow the adhesive to cure before they were unclamped.

12 Each single-bolt single-lap joint was fabricated using a 10 mm diameter bolt with a smooth shank slightly longer
13 than twice the half-lap thickness. A standard steel washer was used under the bolt head and nut. Prior to
14 insertion of the bolt, the laps were aligned co-linearly and clamped. The bolt was then torqued to 3 Nm with a
15 calibrated torque wrench and the co-linearity of the laps was checked.

16 5. Test procedure

17 The ambient temperature single-bolt single-lap joint tension tests were carried out in an Instron 8802 servo-
18 hydraulically controlled test machine (see Figure 1(b)). The elevated temperature tests were carried out in the
19 temperature controlled cabinet positioned between the upper and lower hydraulic grips of the test machine. Each
20 of the latter grips was connected by a circular cross-section steel rod to a 100 kN capacity mechanical grip
21 inside the temperature cabinet. Each rod, passed through a pair of removable, semi-circular annuli. The close-
22 fitting, insulated annuli prevented heat loss from the top and bottom of the temperature cabinet. The bolt torque
23 for the mechanical grips was determined in accordance with machine's guidelines, based on the anticipated joint
24 failure load. The bolts were torqued sequentially until they achieved the prescribed torque, so that the joints
25 could be failed under displacement control. Figure 3 shows details of the elevated temperature test setup based
26 around the Instron test machine and a joint clamped between the mechanical grips inside the temperature cabinet
27 prior to testing.

28 The procedure for the ambient temperature joint tests was rapid and straightforward once each joint had been
29 centred and checked for verticality between the grips of the test machine. The tensile load was applied under
30 displacement control at a rate of 2 mm/minute with both load and extension recorded at 0.1 second intervals. In
31 order to record the failure load and its associated overall extension, the test machine was programmed to cease
32 loading when either the load dropped by 40% or the extension exceeded 10 mm. The procedure for the elevated
33 temperature joint tests was similar, but setup time was much longer. After checking the joint's bolt torque and
34 aligning and clamping the joint between the mechanical grips, which took several minutes, the temperature
35 cabinet was closed and the test temperature set. The joint was then allowed to *soak* at this temperature for at
36 least 20 minutes. This time period has been shown to be sufficient for the joint to achieve the test temperature
37 (Turvey and Wang, 2007b).

38 After completing each test, the joint was removed from the grips and unbolted so that it could be inspected
39 visually. Digital images were made of its failure mode and added to an image gallery.

40 6. Single-bolt single-lap joint tension tests – mean ultimate loads and extensions

41 Six nominally identical joints were tested to failure in tension for each of the twenty [E/D, °C] parameter
42 groups. From the load versus overall extension data recorded for each joint test of each parameter group, the
43 joint's ultimate load and extension were determined. Hence, the mean loads and overall extensions together with
44 their standard deviations could be determined for that group of joints. In several joint groups it was found that
45 one of the joints had an ultimate load or extension inconsistent with those of the rest of the group and was
46 discounted in determining the mean ultimate load and overall extension for that group. Mean cross-sectional
47 areas, ultimate loads and extensions of each joint group are given in Table 4 together with their E/D ratios and
48 test temperatures.

49 The reasons for the inconsistencies in ultimate loads and ultimate extensions of some of the tension joints were
50 not obvious and may not be attributable to a single cause. Excessive extensions to failure could be caused by
51 slip in one or other of the mechanical grips or initiation of adhesive debonding between the packing and the end
52 of the lap. Likewise, inconsistent ultimate loads could be due to differences in the modes of failure. As is

1 evident from Table 5, not all of the joints in a particular [E/D, °C] parameter group exhibited the same dominant
2 failure mode. There may well be other reasons for the inconsistencies in the ultimate loads and extensions.
3 However, in the absence of factual evidence, the Authors do not feel that it is sensible to engage in further
4 speculation.

5 **7. Joint failure modes**

6
7 After each single-bolt single-lap joint had been tested to failure and allowed to cool (elevated temperature tests
8 only) it was released from the test machine's grips. The bolt was then removed so that the joint could be
9 inspected visually to identify the failure mode(s). Digital images were made of both faces of each lap and added
10 to an image gallery for future reference. Table 5 summarises the *dominant* failure modes and Figure 4 depicts
11 examples of these modes. For some joints other types of failure were also evident. For example, net tension was
12 observed in conjunction with cleavage failure and in other instances bearing failure was observed with cleavage,
13 tension and shear failure.

14
15 A few images of the failure modes of the particular joints highlighted in bold in Table 5 are shown in Figure 4.

16 **8. Mean ultimate stresses and overall strains of single-bolt single-lap joints**

17
18 Knowledge of the ultimate stresses that bolted joints may sustain in practice is useful for structural engineers in
19 making preliminary assessments of their joint designs. Therefore, the failure loads of each of the single-bolt
20 single-lap joints tested have been divided by their mean cross-sectional areas to obtain their ultimate stresses
21 and the mean and standard deviations of the five/six valid ultimate stresses for each (E/D, °C) parameter group
22 of nominally identical joints have been calculated. These mean stresses are plotted in Figure 5 as functions of
23 the E/D ratio for each test temperature. It is evident that the highest ultimate stresses are obtained under ambient
24 temperature test conditions and that the ultimate stresses reduce as the test temperature increases. It is also
25 apparent that the mean ultimate stress increases as the E/D ratio increases from 2 to 2.5/3 and then remains
26 roughly constant with further increase in the E/D ratio. Moreover, the largest and smallest increases in ultimate
27 stress for the E/D = 2 – 2.5/3 ratios apply to the 20 and 80 °C test temperatures, respectively.

28
29 It is helpful to present the alternative data plot, namely mean ultimate stress as a function of the test temperature
30 for the five E/D ratios, as shown in Figure 6. It is evident that the mean ultimate stress decreases as the test
31 temperature increases. Joints with E/D = 2 have the smallest reduction in ultimate stress over the temperature
32 range. And for joints with E/D > 2 tested at 40 °C and above the ultimate stresses are similar and reduce linearly
33 with increasing temperature.

34
35 Although of less practical significance than joint ultimate stresses, it is of interest to quantify and correlate the
36 overall strains of the joints with their corresponding ultimate stresses. Hence, for each of the five/six nominally
37 identical joints in each (E/D, °C) parameter group its overall strain at failure has been calculated by dividing its
38 overall extension by twice the lap length (2L). From these values, the mean overall strain and standard deviation
39 for the group of joints has been determined. The mean overall ultimate strains are shown in Figure 7 as
40 functions of the E/D ratio for each test temperature. The general shapes of the curves bear similarities with those
41 shown for ultimate stresses in Figure 5. However, there are a number of differences. Whereas, in Figure 5 the
42 highest ultimate stresses correspond to the lowest test temperature, the highest ultimate strains apply to the
43 highest test temperature. Somewhat unexpected is the fact that for E/D > 3 the ultimate strains for the 40 °C test
44 temperature are lower than those for the 20 °C temperature. Another, unanticipated, feature is that, for the 60 °C
45 test temperature, the ultimate strains increase throughout the E/D range, whereas for each of the other three
46 temperatures the corresponding strains are roughly equal for E/D > 3. There is/are no obvious explanation(s) for
47 these unexpected features. They may, in part, be due to the simplistic approach used to calculate the overall
48 ultimate strain. The use of strain gauges or mechanical extensometers in the vicinity of the bolt may have
49 enabled accurate determinations of the local strains at failure, but, in the case of strain gauges, would have
50 significantly increased costs. It is also possible that through-thickness damage at the edge of the bolt holes
51 caused by bolt rotation may have affected the overall extensions at failure. Furthermore, it appears that bolt
52 rotation may reduce as E/D increases. It must be recognised that these tentative reasons for the unexpected
53 observations are nothing more than speculation and that additional, more comprehensively instrumented tests,
54 would be required to give them credence.

55
56 The overall mean ultimate strains are plotted as functions of test temperature for each of the five E/D ratios in
57 Figure 8. It appears that for E/D = 2 and 2.5 the ultimate strains increase linearly with increasing temperature
58 and that the latter strains are greater than the former throughout the temperature range. However, for E/D = 3 –
59
60
61
62
63
64
65

5, the trends are less clear, though, for the 20, 40 and 80 °C temperatures, the overall mean ultimate strains are of similar magnitude. However, the strains for 40 °C are lower than for 20 °C and for 60 °C the difference between the ultimate strains is relatively large.

9. Characteristic stresses and overall strains of single-bolt single-lap tension joints

For joint design it is important to know characteristic values of relevant properties, especially characteristic stresses and strains. According to Annexe D of BS EN 1990 the characteristic value of a relevant design quantity, may be determined from test data using the following simple relationship:-

$$\sigma_c = \sigma_m - k\sigma_{sd} \quad (1)$$

In Eq. (1) σ_c denotes the characteristic value of the design quantity, σ_m is the mean value of the same quantity, σ_{sd} is its standard deviation and k is a constant which depends on the number of nominally identical values of the quantity determined by testing. In the present investigation six nominally identical joints were tested to failure in each (E/D, °C) parameter group. Therefore, according to Annexe D, the value of k in Eq. (1) is 1.77. However, in several of the parameter groups only five of the nominally identical joints tested gave valid results; consequently, in accordance with Annexe D, the value of k increases to 1.80. The mean ultimate stresses and associated standard deviations of each of the 20 parameter groups were processed in accordance with Eq. (1) to determine the characteristic stresses for the single-bolt single-lap tension joints, as given in Table 6. Design ultimate stresses may then be determined by dividing the characteristic stresses by material factors, which are generally greater than unity and depend on the particular circumstances/environmental conditions in which the joints have to function.

Eq. (1) has also been used in a similar manner to determine the characteristic overall ultimate strains, given in Table 7, for the single-bolt single-lap tension joints.

10. Knock-down factors for characteristic ultimate stresses of single-bolt single-lap tension joints and comparison with knock-down factors of single-bolt double-lap joints

It is well known that bolted joints are often the weakest links in structures. Moreover, it is expected that the ultimate stress that a bolted joint may sustain is much less than that of the virgin or parent material under the same loading and environmental conditions. Furthermore, it is recognised that, for tension joints, the ultimate stress of the double-lap configuration is generally greater than that of the single-lap configuration, because of the absence of tension induced flexure prior to joint failure as a consequence of lap eccentricity. Therefore, it is of interest to quantify the reductions in ultimate stress, compared to that of the virgin material, for the 20 parameter groups of joints. The reduction in ultimate stress may be expressed either in percentage terms (efficiencies) or knock-down factors. Here the latter have been chosen, so that comparisons may also be made with similar factors for single-bolt double-lap tension joints (Turvey and Sana, 2016). Knock-down factors are simply expressed as the value of the joints' ultimate stresses divided by the virgin material's ultimate stress. Ideally, four virgin material's ultimate stresses should be available – one for each test temperature. Unfortunately, only the virgin material's ultimate stress at ambient temperature (20 °C) was available. Hence, the knock-down factors presented for the 40 – 80 °C temperatures are likely to be lower bounds and, therefore, conservative. The knock down factors for the 20 parameter groups of joints are presented in Tables 8 and 9.

For a given temperature, it is evident that the knock-down factors for both the mean ultimate and characteristic mean ultimate stresses increase with increasing E/D ratio. Moreover, they decrease with increasing temperature for a given E/D ratio. However, for each temperature and E/D > 2.5 the knock-down factors remain roughly constant.

As already mentioned, knock-down factors for the mean ultimate stresses of single-bolt double-lap tension joints were reported recently (Turvey and Sana, 2016) and can be compared with those in Table 8. The comparison is presented for E/D = 2 - 5 in Figure 9.

It is evident that in Figure 9(a) the knock-down factors for the single-bolt double-lap joints increase as the E/D ratio increases from 2 to 5. The knock-down factors for the 40 °C test temperature are roughly 10% lower than the corresponding factors for the 20 °C temperature. Moreover, for these two temperatures the double-lap

1 knock-down factors range from around 0.2 up to about 0.4, indicating losses in mean ultimate stress capacity of
2 between 80 and 60%, respectively, compared to that of the virgin GFRP plate.

3 On the other hand, the dependency of the knock-down factors on the E/D ratio for single-bolt single-lap tension
4 joints differs somewhat from that of the corresponding double-lap joints. It increases gradually from 2 up to 2.5/3
5 and then remains constant with further increase in the ratio. Furthermore, for the single-lap joints the knock-
6 down factors for the 40 °C temperature are significantly lower than those for the 20 °C temperature, being about
7 25% lower for E/D = 3 – 5.

8
9 Turning now to the knock-down factors for the 60 and 80 °C test temperatures, shown in Figure 9(b), the
10 double-lap knock-down factors gradually increase up to an E/D ratio of 4 before starting to level off or decrease
11 slightly. However, the values are significantly lower than those for the 20 and 40 °C test temperatures. The 80
12 °C knock-down factors are lower than the corresponding 60 °C factors. Moreover, the knock-down factors for
13 the single-lap joints are constant for E/D ratios of 2.5 – 5 and very low, being about 0.19 for the 60 °C and 0.16
14 for the 80 °C test temperature, respectively. However, the 20 °C temperature difference between the latter two
15 test temperatures only reduces the knock-down factor by about 16%, whereas for the same temperature
16 difference between the 20 and 40 °C temperatures the reduction in the knock-down factor is significantly larger,
17 amounting to 25% (see Figure 9(a)). These observations are expected, since (as shown in Figure 5) the reduction
18 in mean ultimate stress for E/D > 3 is significantly greater between the 20 and 40 °C test temperatures than
19 between the 60 and 80 °C test temperatures.
20

21 **11. Concluding remarks**

22
23 The investigation, described herein, involved testing 120 single-bolt single-lap pultruded GFRP joints to failure
24 in uni-axial tension. The joints were sub-divided into 20 parameter groups, each comprising six nominally
25 identical joints. These parameter groups (with five E/D ratios, four test temperatures and six nominally identical
26 joints per group) enabled the effects of joint geometry and test temperature on mean values and standard
27 deviations of ultimate loads and overall extensions to be quantified. The data has also been used to calculate
28 mean ultimate stresses/overall strains and corresponding characteristic values. In addition, knock-down factors
29 for mean ultimate stress have been determined relative to the 20 °C mean ultimate stress of the virgin pultruded
30 GFRP plate from which the joints were fabricated. All of the data is applicable to a single W/D ratio and steel
31 bolt diameter.
32

33 The mean ultimate stress has been shown to reduce with increasing temperature and, for each test temperature,
34 to be reasonably constant for E/D ratios greater than 3. Moreover, it has also been shown to reduce almost
35 linearly with temperature with the smallest overall reduction for the lowest E/D ratio. Furthermore, for
36 temperatures above 40 °C the joints' ultimate stresses appear to follow the same linear reduction with increasing
37 temperature for all E/D ratios.
38

39 Unsurprisingly, discernible trends for the overall mean ultimate strains were difficult to identify. It appears that
40 at the higher test temperatures (60 and 80 °C) they increase with increasing E/D ratio, whereas for the lower
41 temperatures (20 and 40 °C) the strains increase initially and then tend to constant values above E/D = 2.5/3.
42 Counter-intuitively, the overall mean ultimate strains for the 20 °C test temperature exceed those for the 40 °C
43 test temperature. The overall mean ultimate strains tend to increase linearly with increasing temperature for E/D
44 = 2 and 2.5. For larger E/D ratios the variation with temperature does not quite follow the latter trend, though
45 there is some evidence that the values are not all that dissimilar for the same E/D ratios.
46

47 Mean characteristic ultimate stresses/overall strains have been determined and tabulated for the range of E/D
48 ratios and test temperatures investigated. The former values, in particular, are potentially beneficial for the
49 preliminary stage of tension joint design, because they permit a rapid assessment of the likely reduction in the
50 design stress for a particular joint geometry and environmental operating temperature, albeit only for single-bolt
51 single-lap joints. Moreover, the comparison of knock-down factors enables a rapid preliminary design
52 assessment to be made of the ultimate stress benefit of using a double-lap rather than a single-lap joint
53 configuration if the design situation permits such a change.
54

55 **Acknowledgements**

56
57 The Authors wish to express their appreciation to Mr. Mark Salisbury for his help and support with the
58 experimental work. They also wish to thank the Engineering Department for providing access to its Structures
59
60
61
62
63
64
65

and Materials Laboratory's test facilities, without which, this research investigation could not have been brought to a successful conclusion.

References

Abd-El-Naby SFM, Hollaway L (1993a) The experimental behaviour of bolted joints in pultruded glass/polyester material. Part 1: Single-bolt joints. *Composites* **24(7)**: 531-538.

Abd-El-Naby SFM, Hollaway L (1993b) The experimental behaviour of bolted joints in pultruded glass/polyester material. Part 2: Two bolt joints. *Composites* **24(7)**: 539-546.

Cooper C, Turvey GJ (1995) Effects of joint geometry and bolt torque on the structural performance of single bolt tension joints in pultruded GRP sheet material. *Composite Structures* **32(1-4)**:217-226.

Hassan NK, Mohamedien MA, Rizkalla SH (1997) Multibolted joints for GFRP structural members. *Journal of Composites for Construction* **1(1)**:3-9.

Rosner C, Rizkalla S (1995) Bolted connections for fiber-reinforced composite structural members: experimental program. *Journal of Materials for Civil Engineering* **7(4)**: 223-231.

Turvey GJ (1998) Single-bolt tension joint tests on pultruded GRP plate – effects of the orientation of the tension direction relative to pultrusion direction. *Composite Structures* **42(4)**: 341-351.

Turvey GJ (2012) Failure of single-lap single-bolt tension joints in pultruded glass fibre reinforced plate. In *6th International Conference on Composites in Construction Engineering (CICE)*, Rome, Italy. [Section 08-089, pp.6 in CD Rom Proceedings].

Turvey GJ (2013) Ultimate loads, strengths, extensions and strains of pultruded GFRP single-lap single-bolt tension joints. In *Proceedings of the 6th International Conference on Advanced Composites in Construction* (Whysall CJ and Taylor SE) Net Composites Ltd, UK, pp. 357-367.

Turvey GJ (2014) An experimental investigation of the failure of pultruded GFRP single-lap two-bolt connections in tension, In *Proceedings of the International Conference, FRP Bridges 2014*, London, UK. [CD Rom Proceedings].

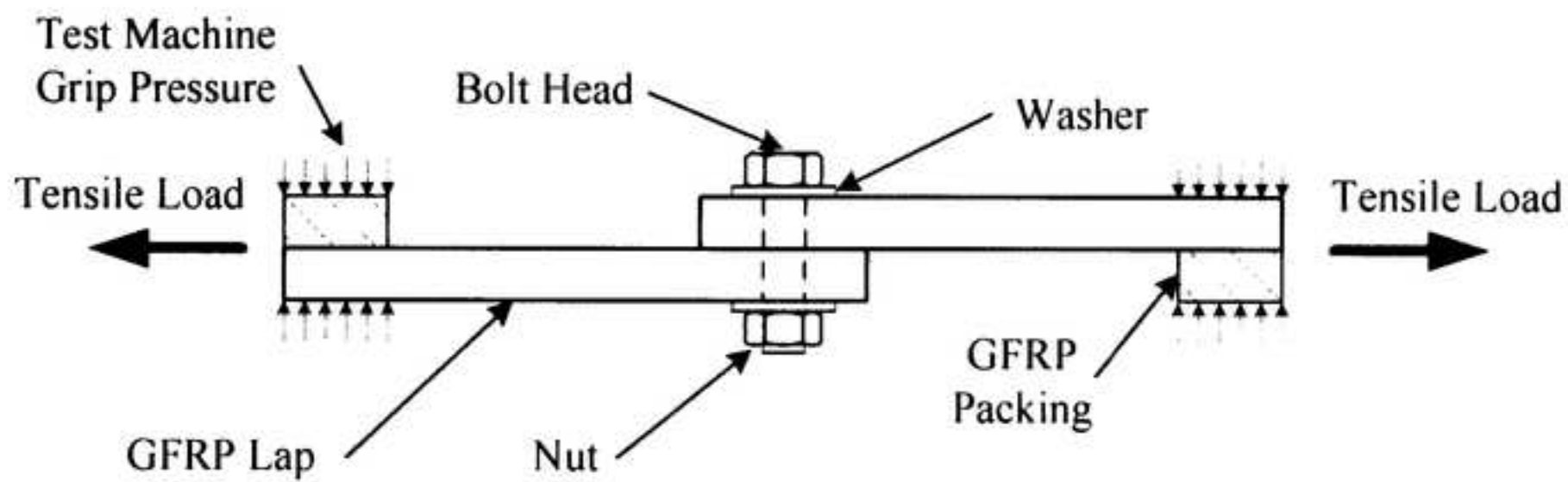
Turvey GJ, Cooper C (1995) Single bolt tension joint tests on pultruded GRP WF-section web and flange material. In *Proceedings of the Tenth International Conference on Composite Materials, Vol III, Processing and Manufacturing*, (Poursartip A and Street K (eds)). Woodhead Publishing Limited, UK pp. 621-628.

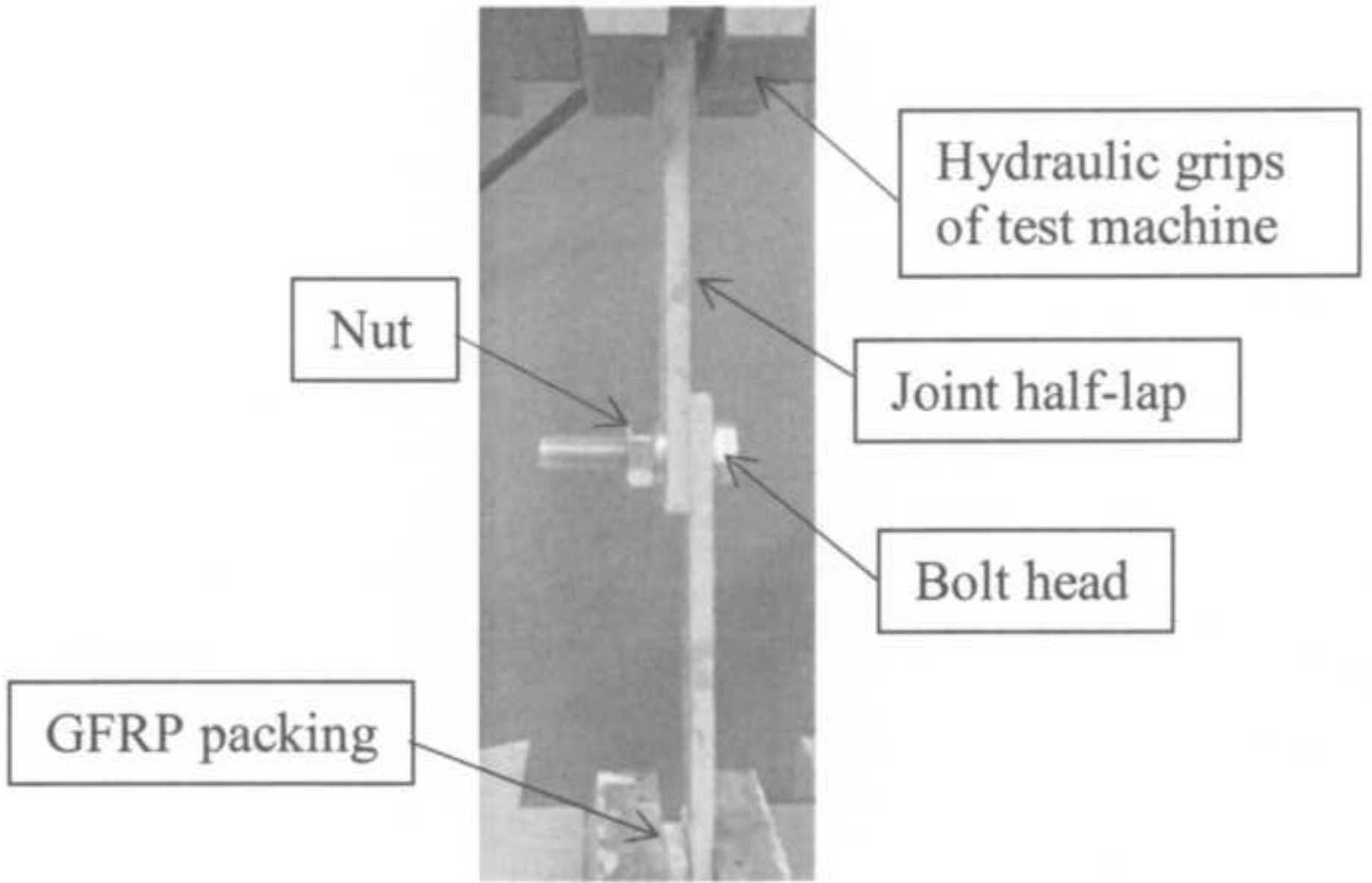
Turvey GJ, Sana A (2016) Pultruded GFRP double-lap single-bolt tension joints – Temperature effects on mean and characteristic failure stresses and knock-down factors. *Composite Structures* **153**: 624-631.

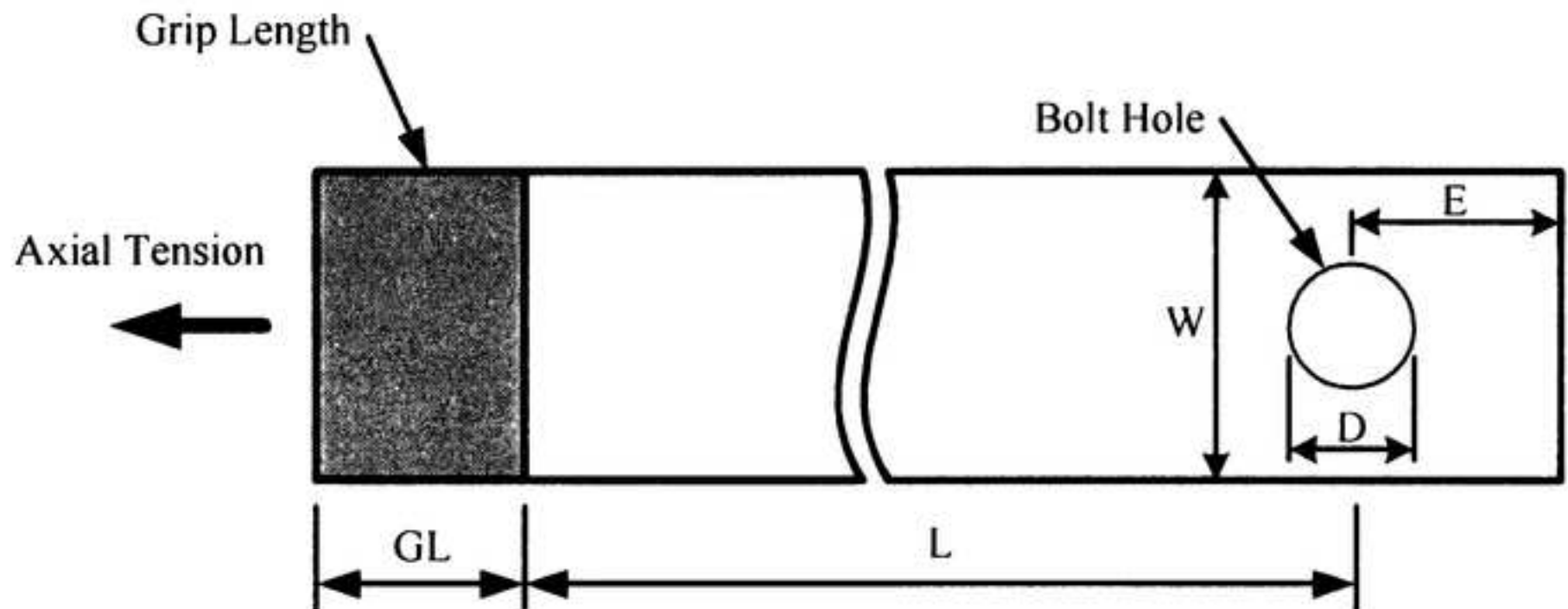
Turvey GJ, Wang P (2007a) Failure of pultruded GRP single-bolt tension joints under hot-wet conditions. *Composite Structures* **77(4)**: 514-520.

Turvey GJ, Wang P (2007b) Thermal preconditioning study for bolted tension joints in pultruded GRP plate. *Composite Structures* **77(4)**:509-513.

Turvey GJ, Wang P (2009) Failure of pultruded GRP bolted joints: a Taguchi analysis. *Proceedings of the Institution of Civil Engineers: Engineering and Computational Mechanics* **162(EM3)**:155-166.









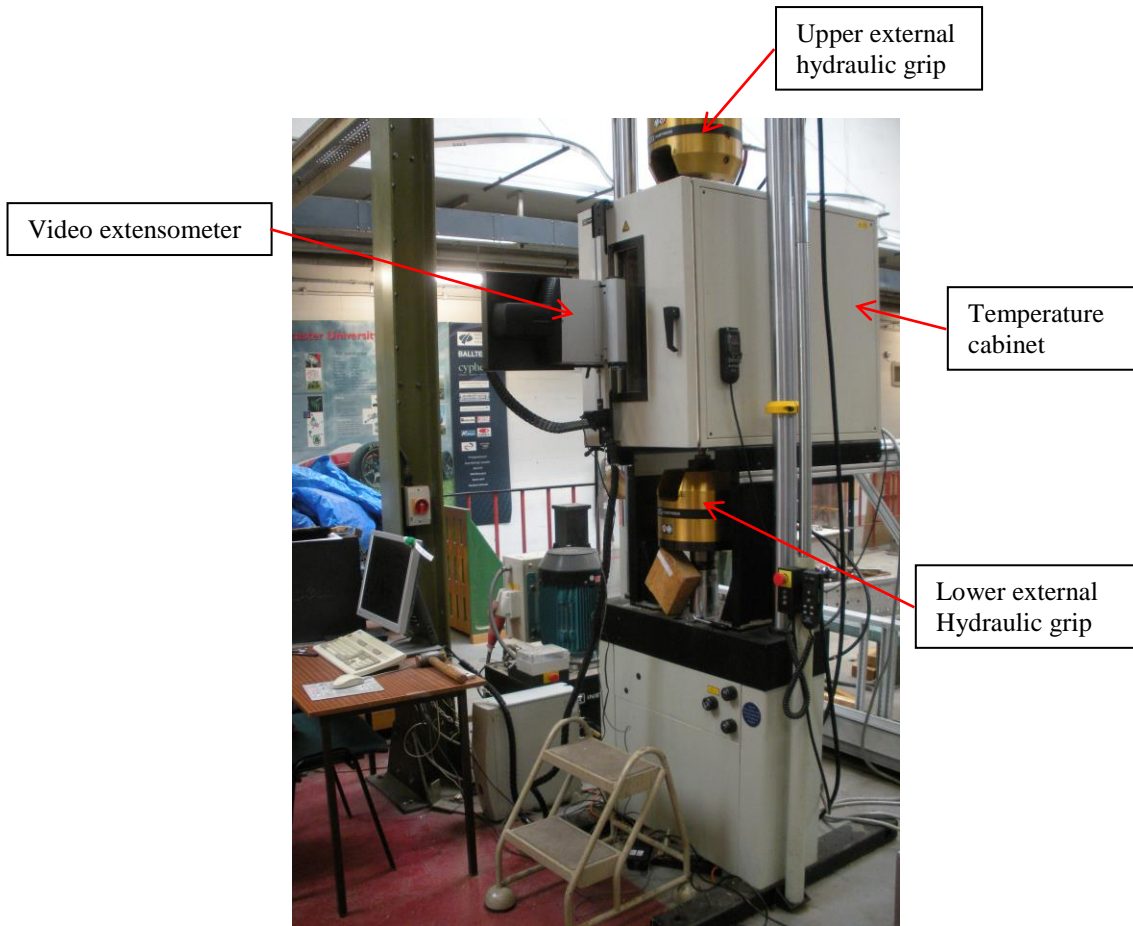


Figure 3(a) rev1 – with labels



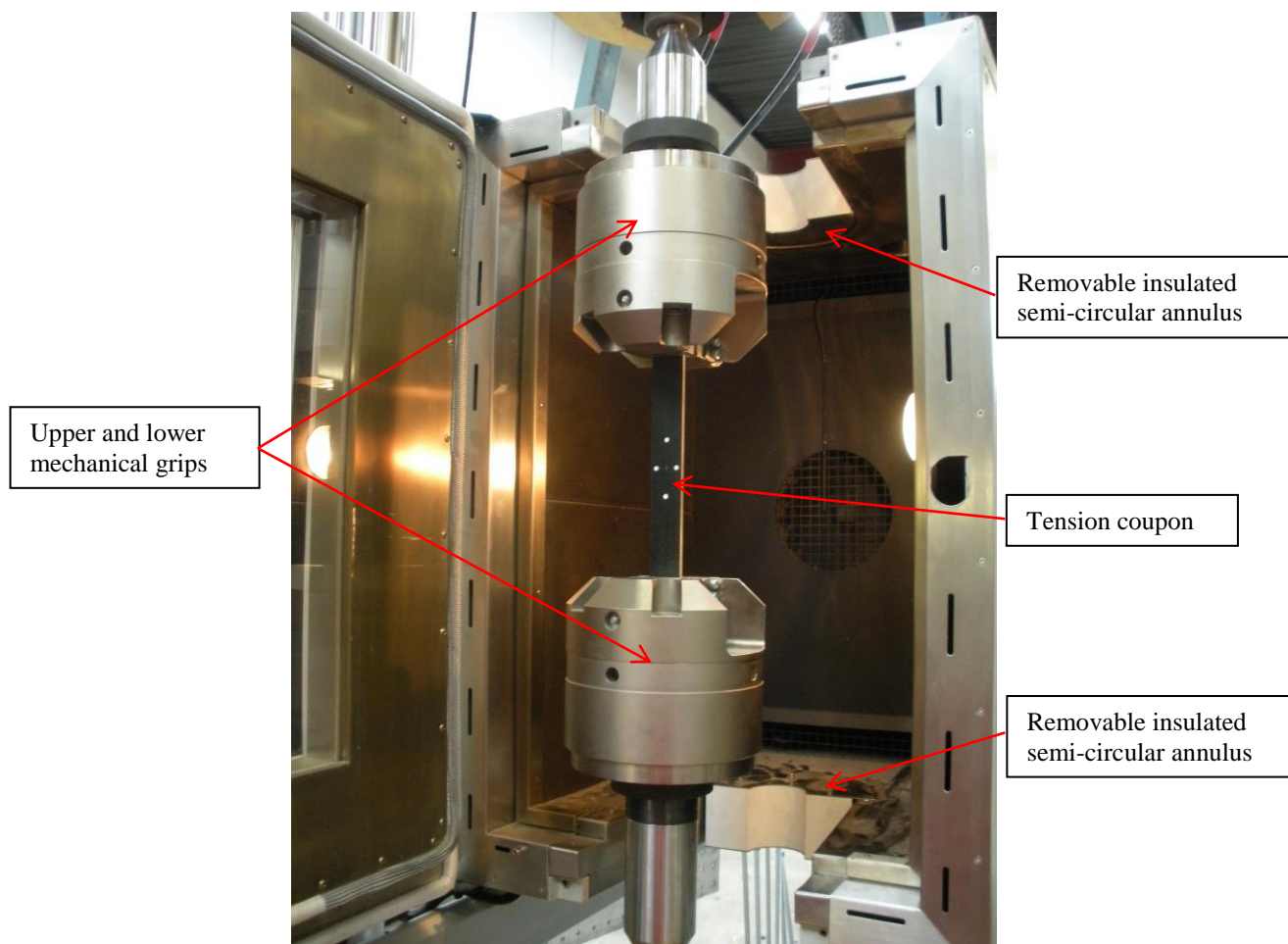


Figure 3(b) – with labels



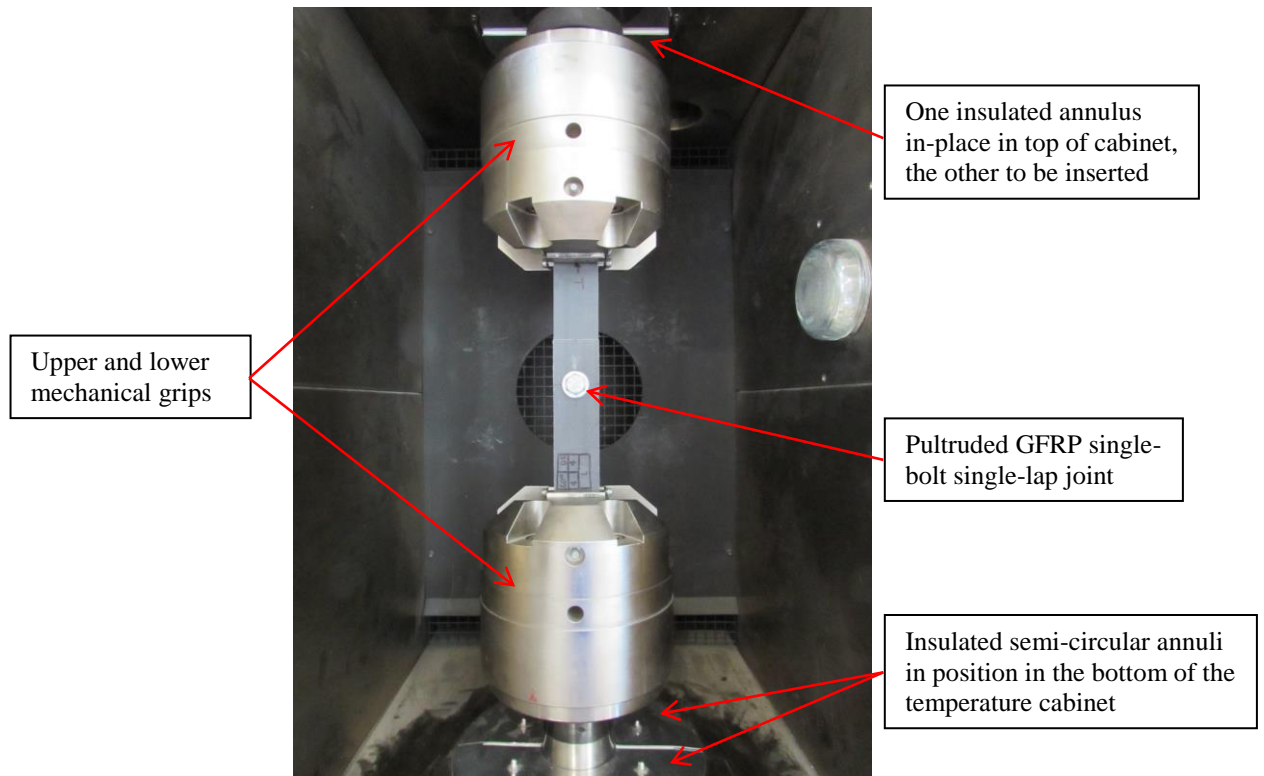
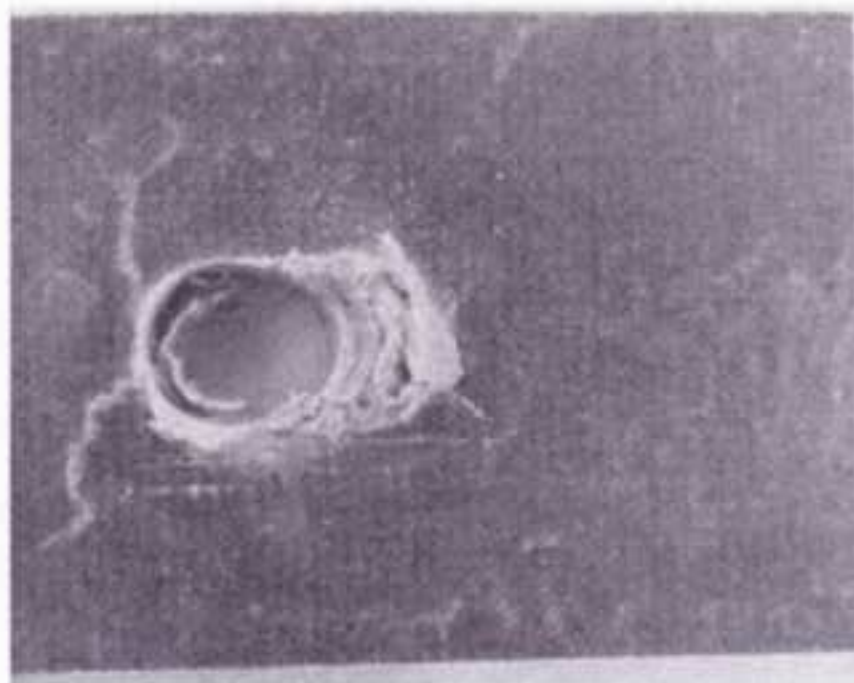
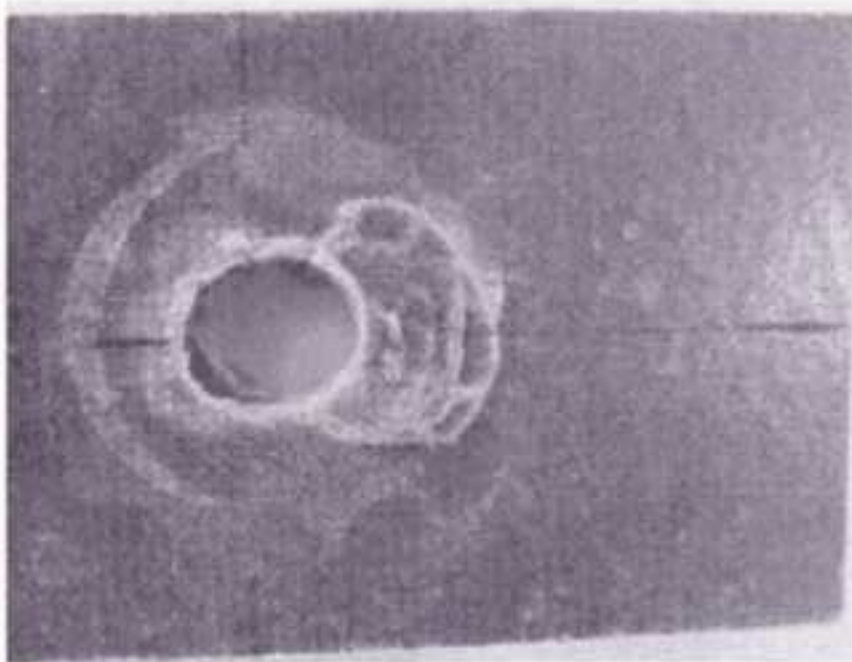
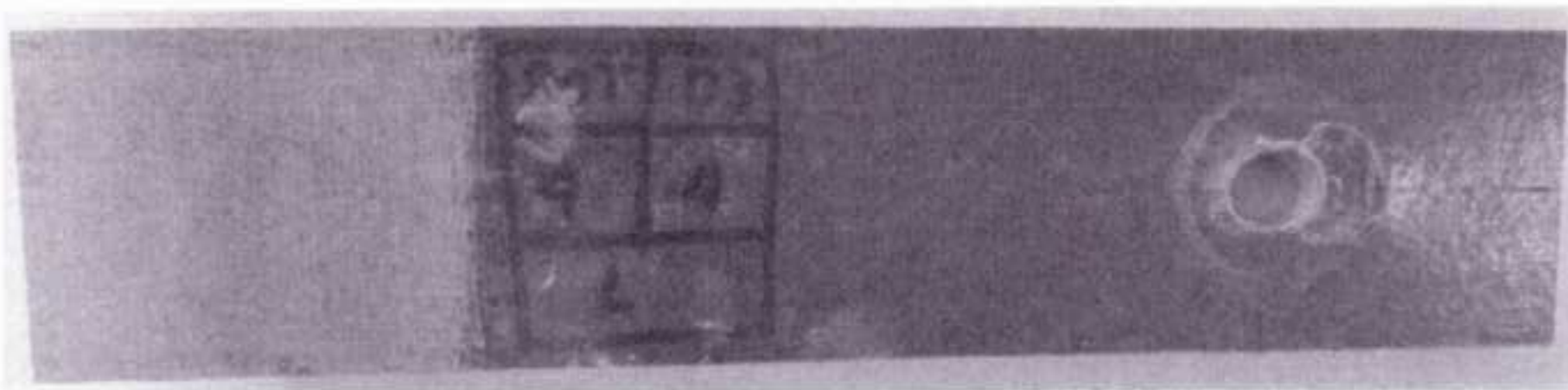
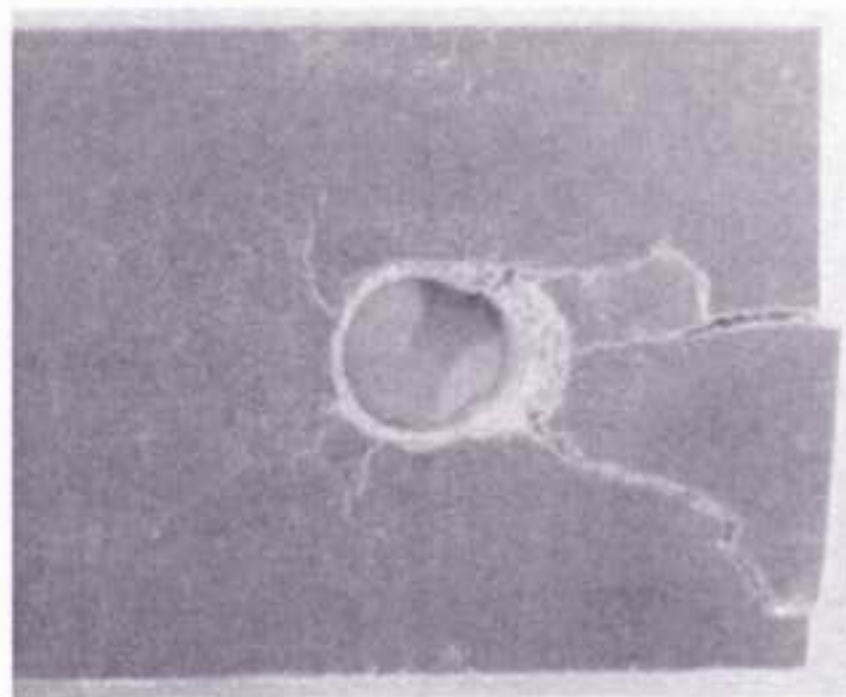
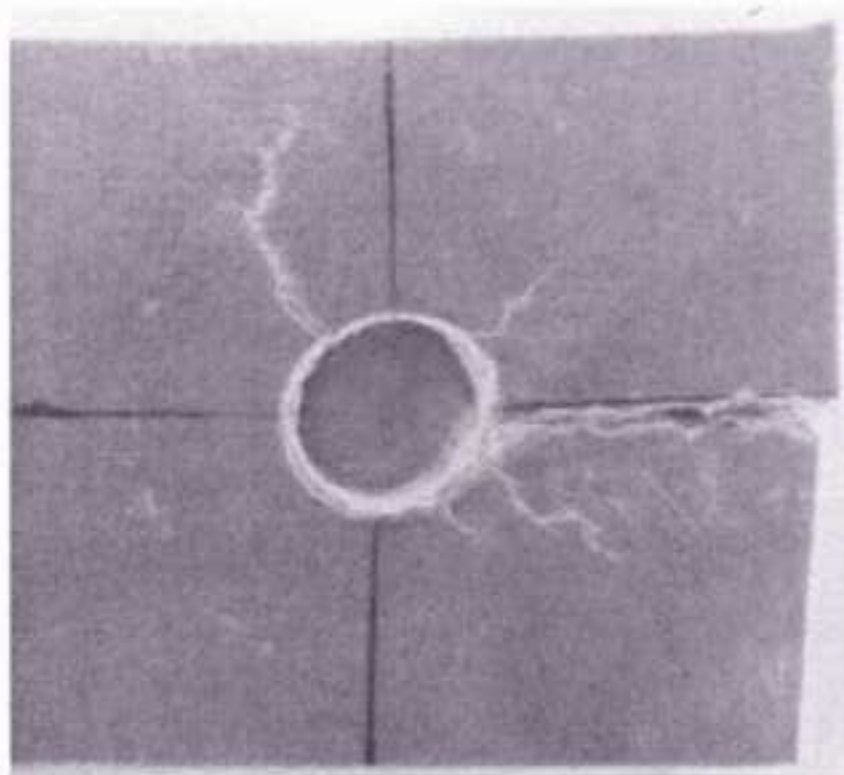
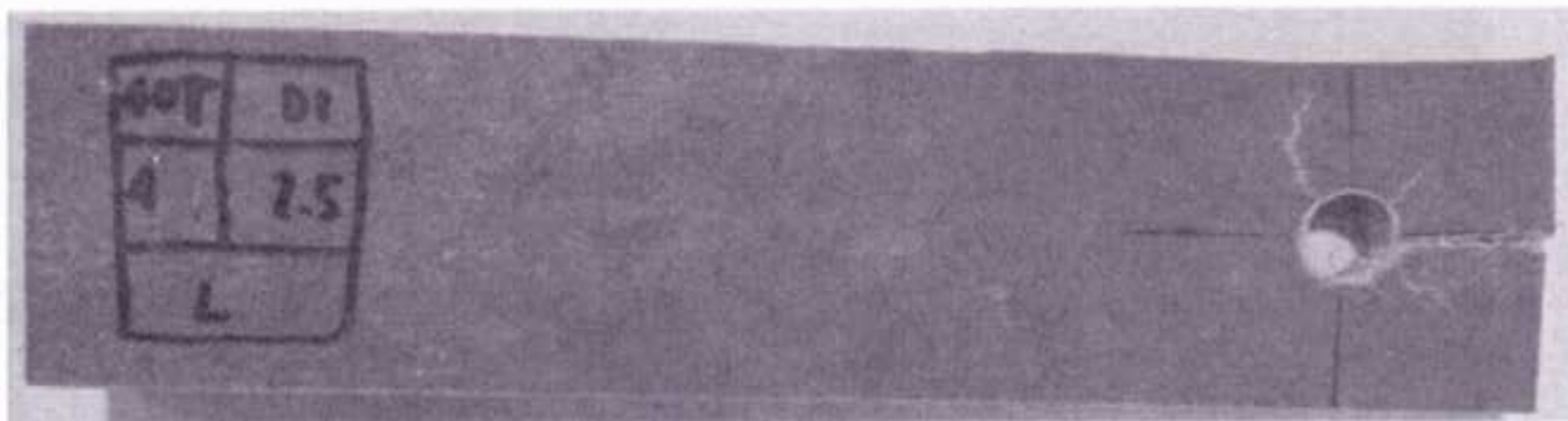
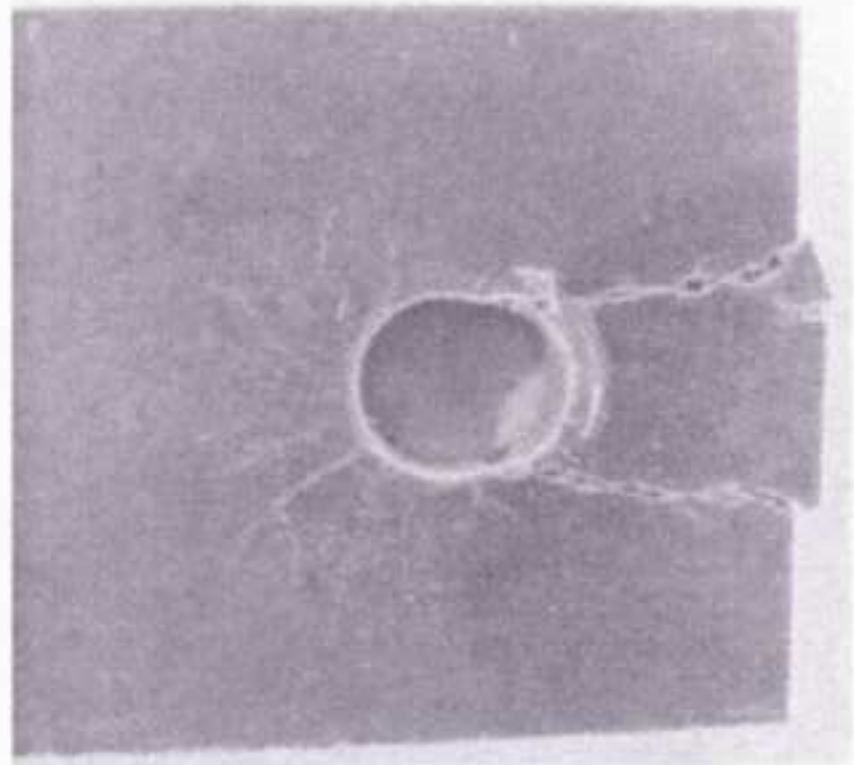
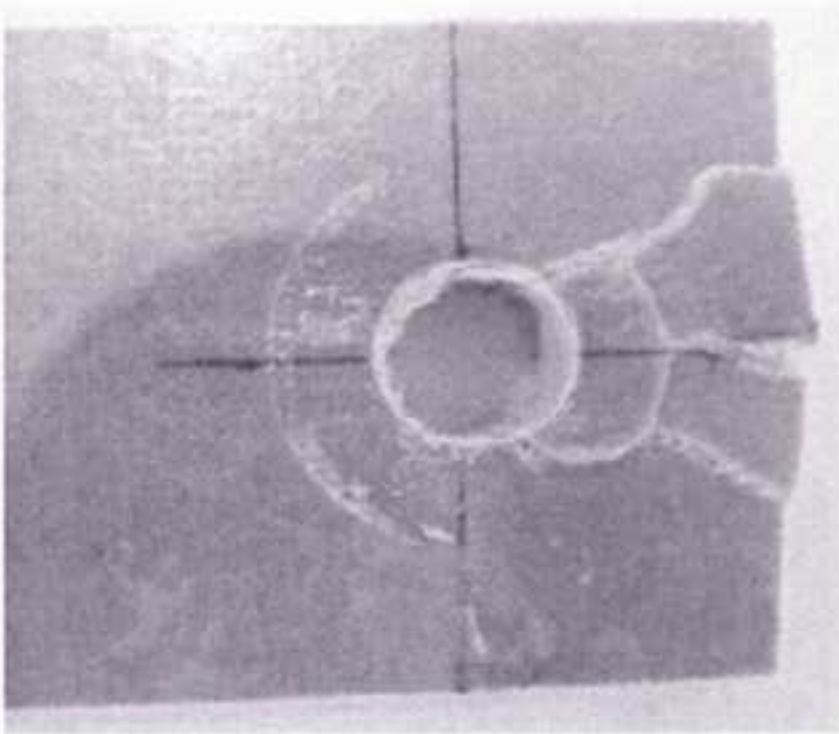
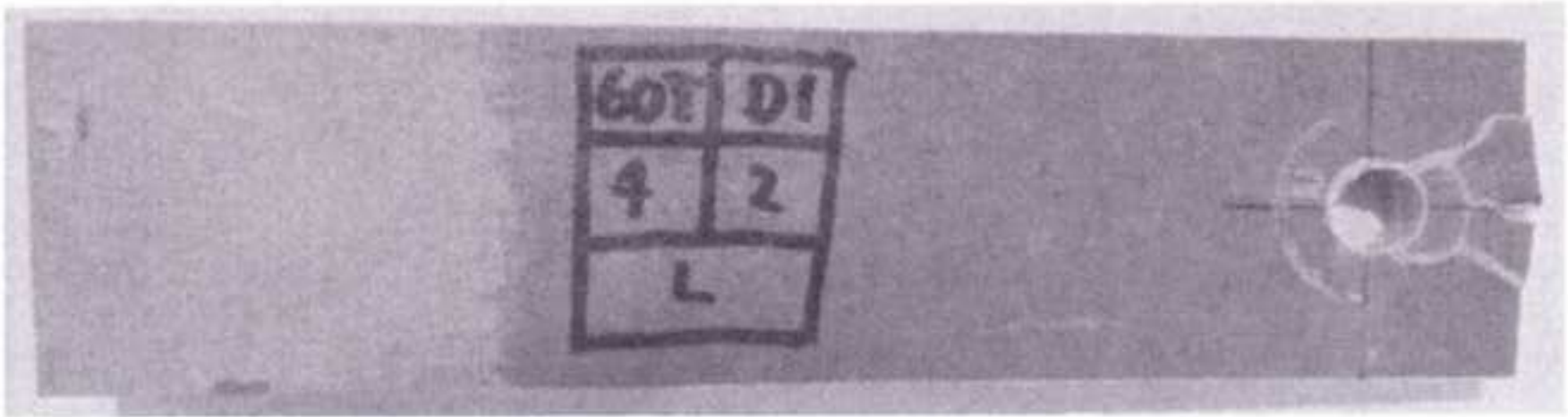
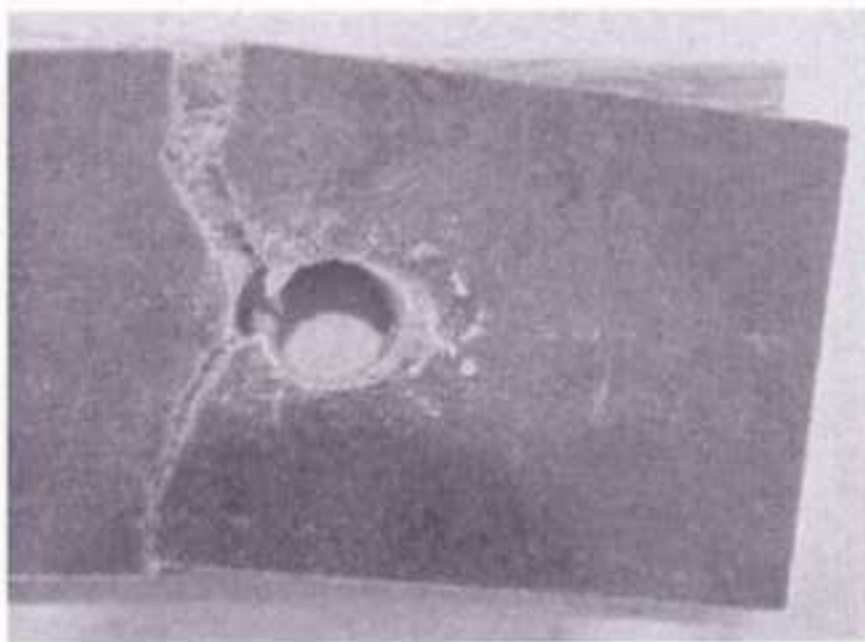
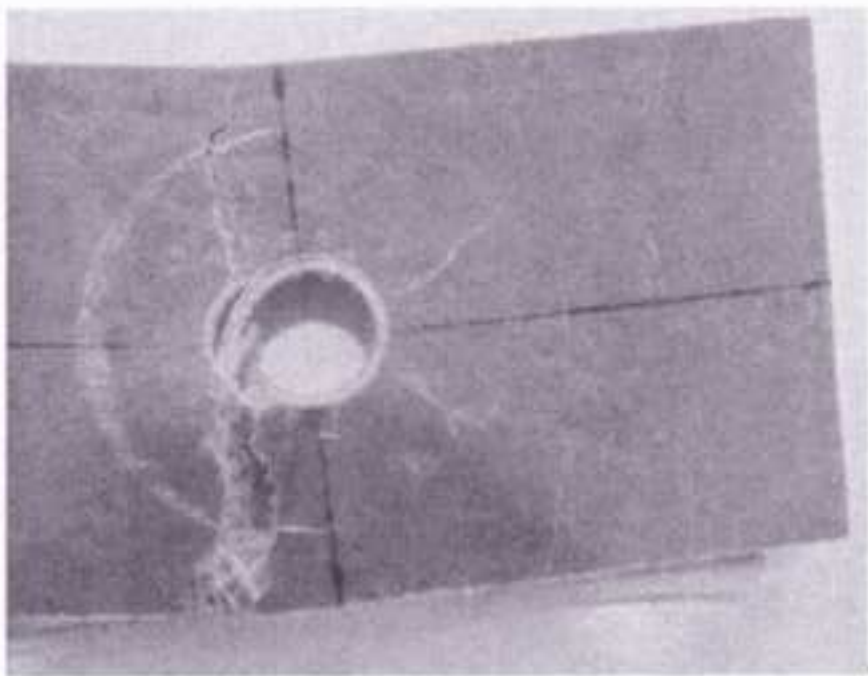
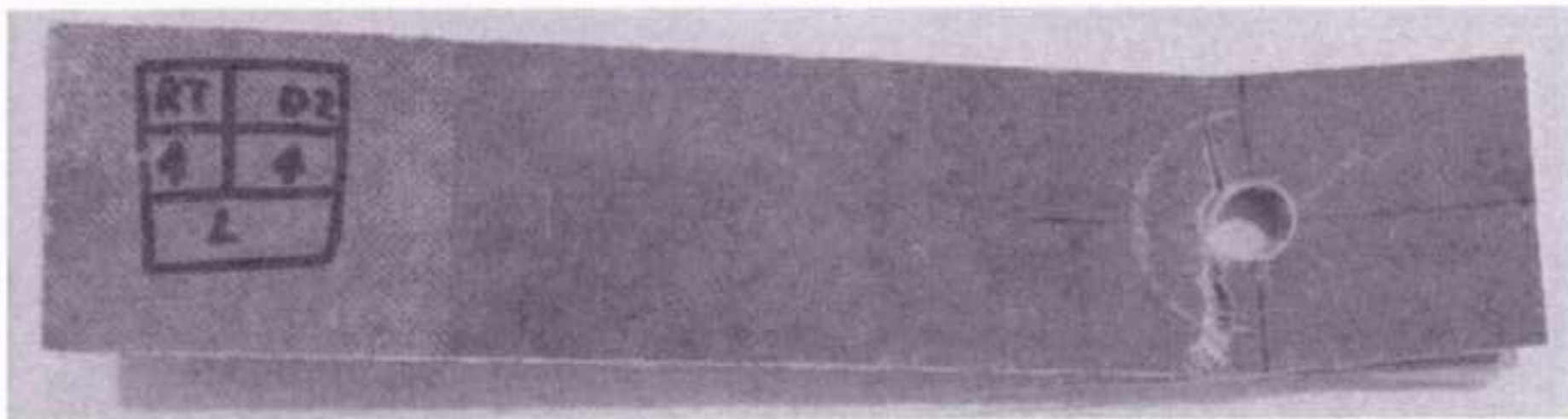


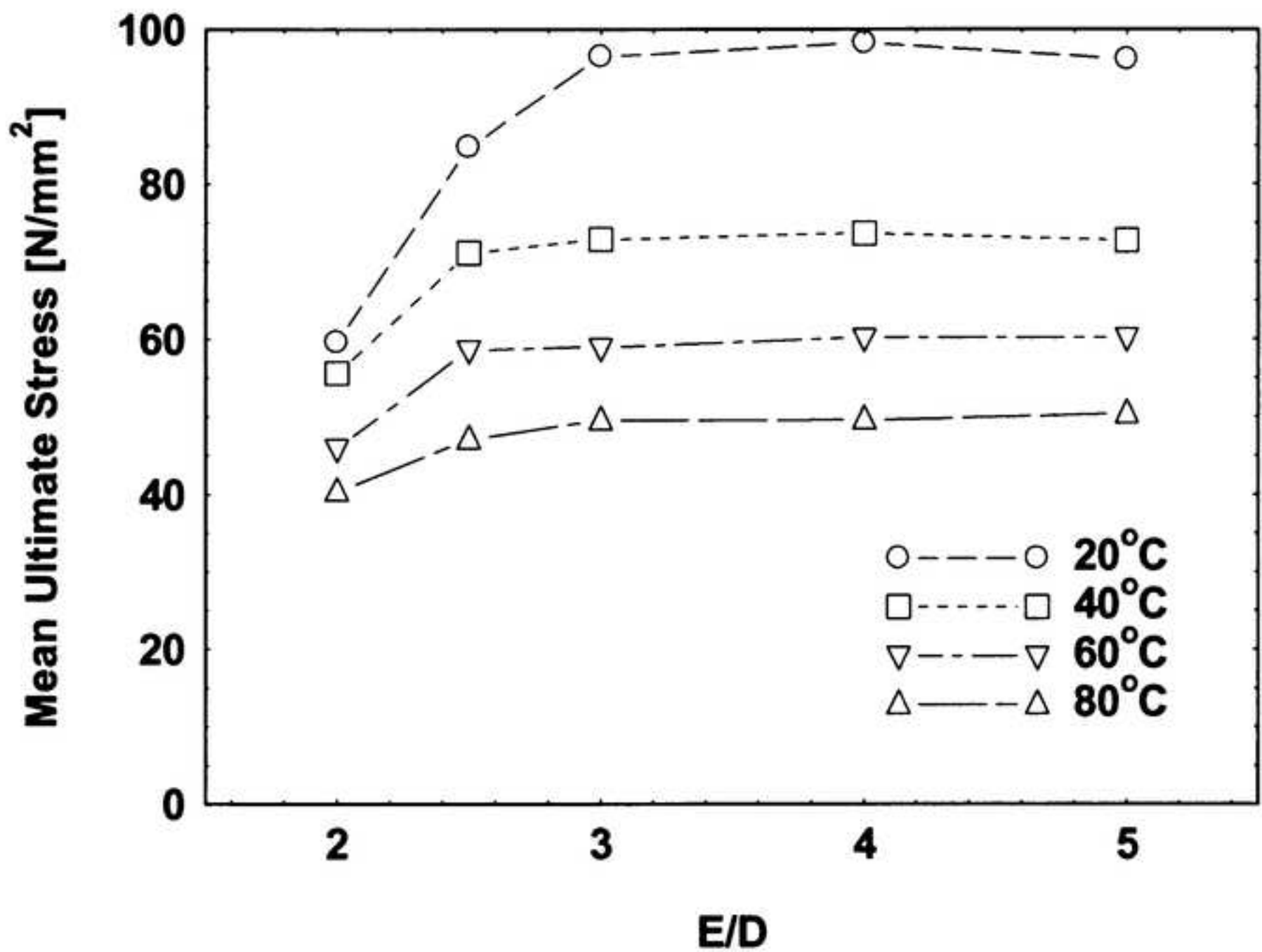
Figure 3(c) – with labels

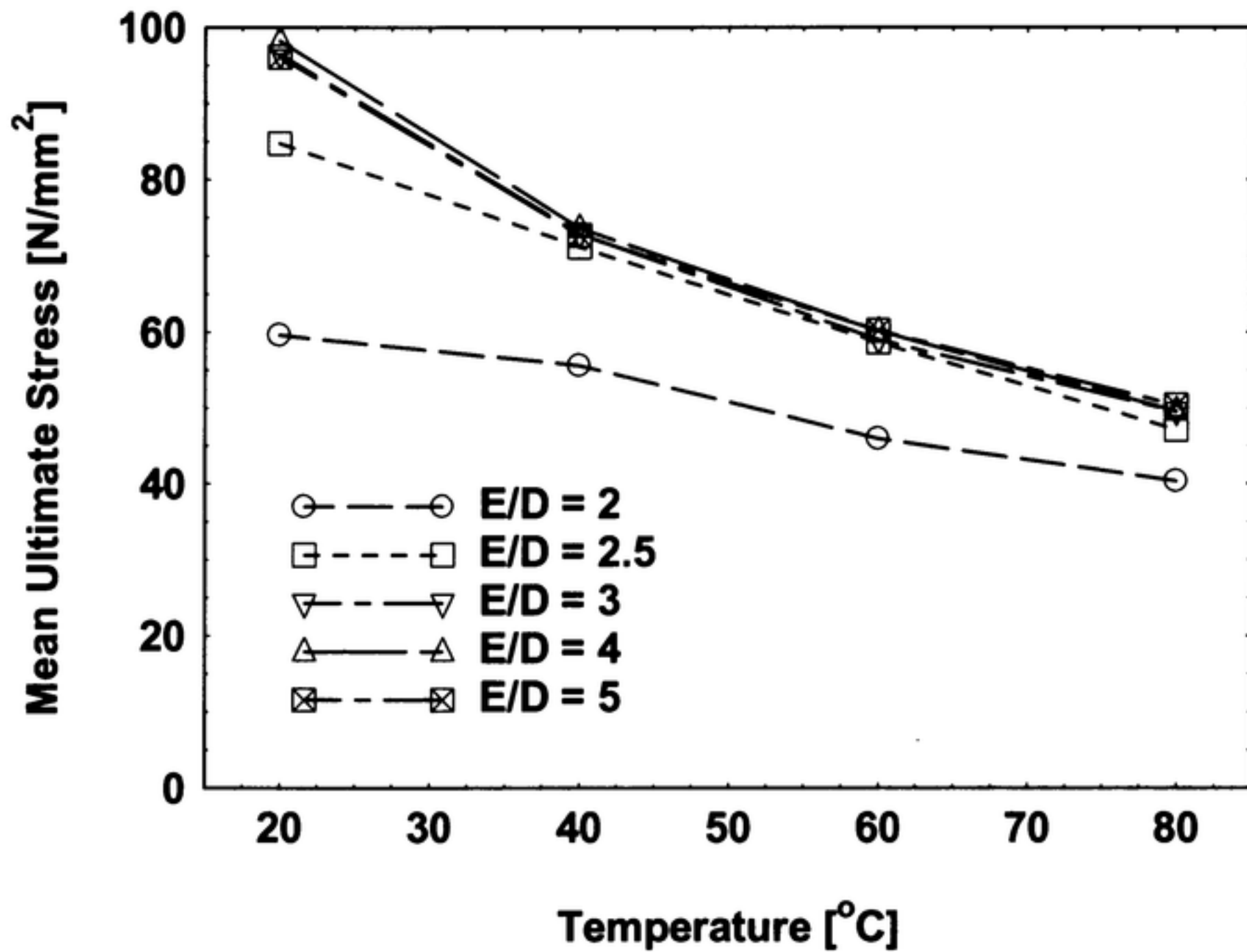


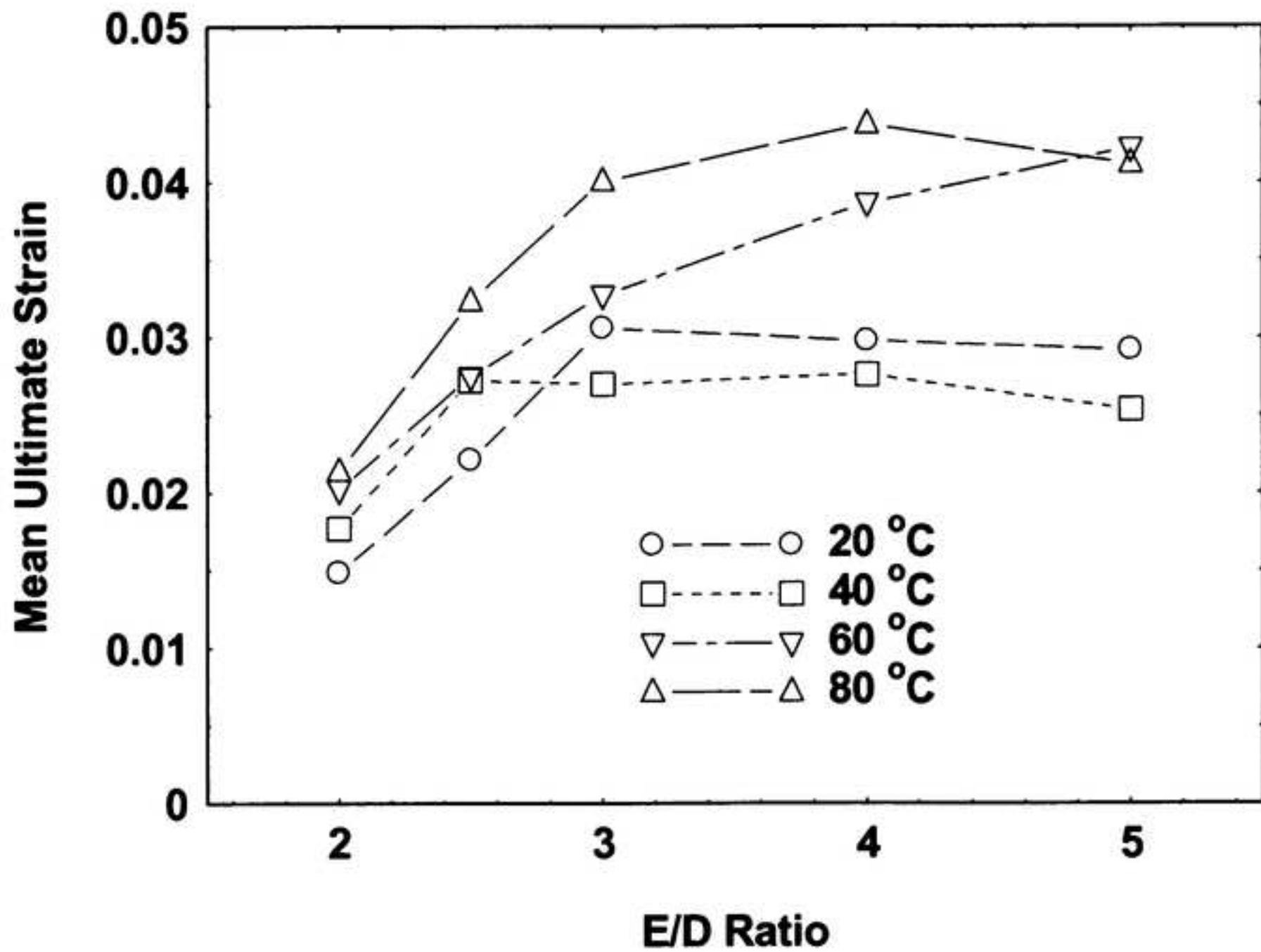


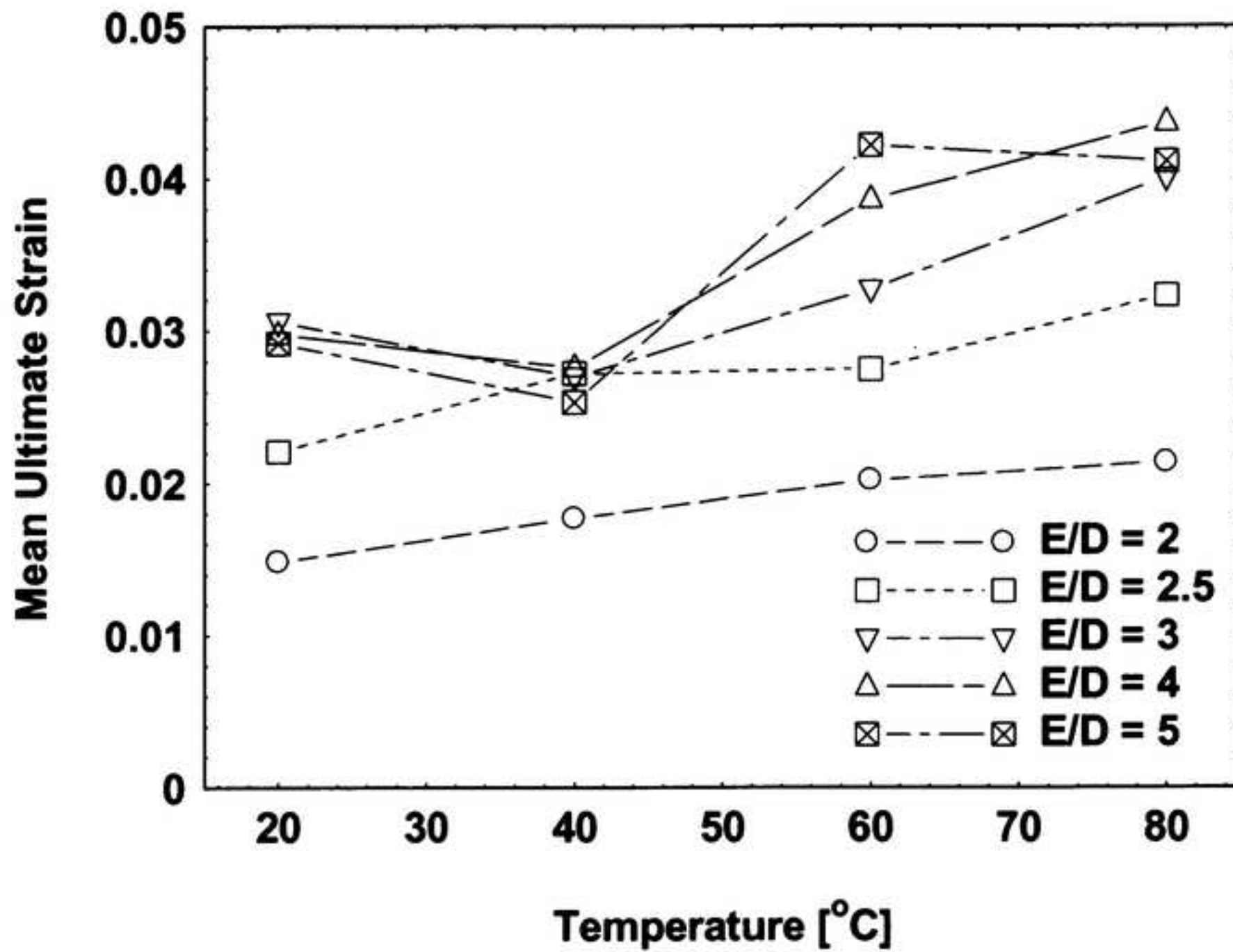


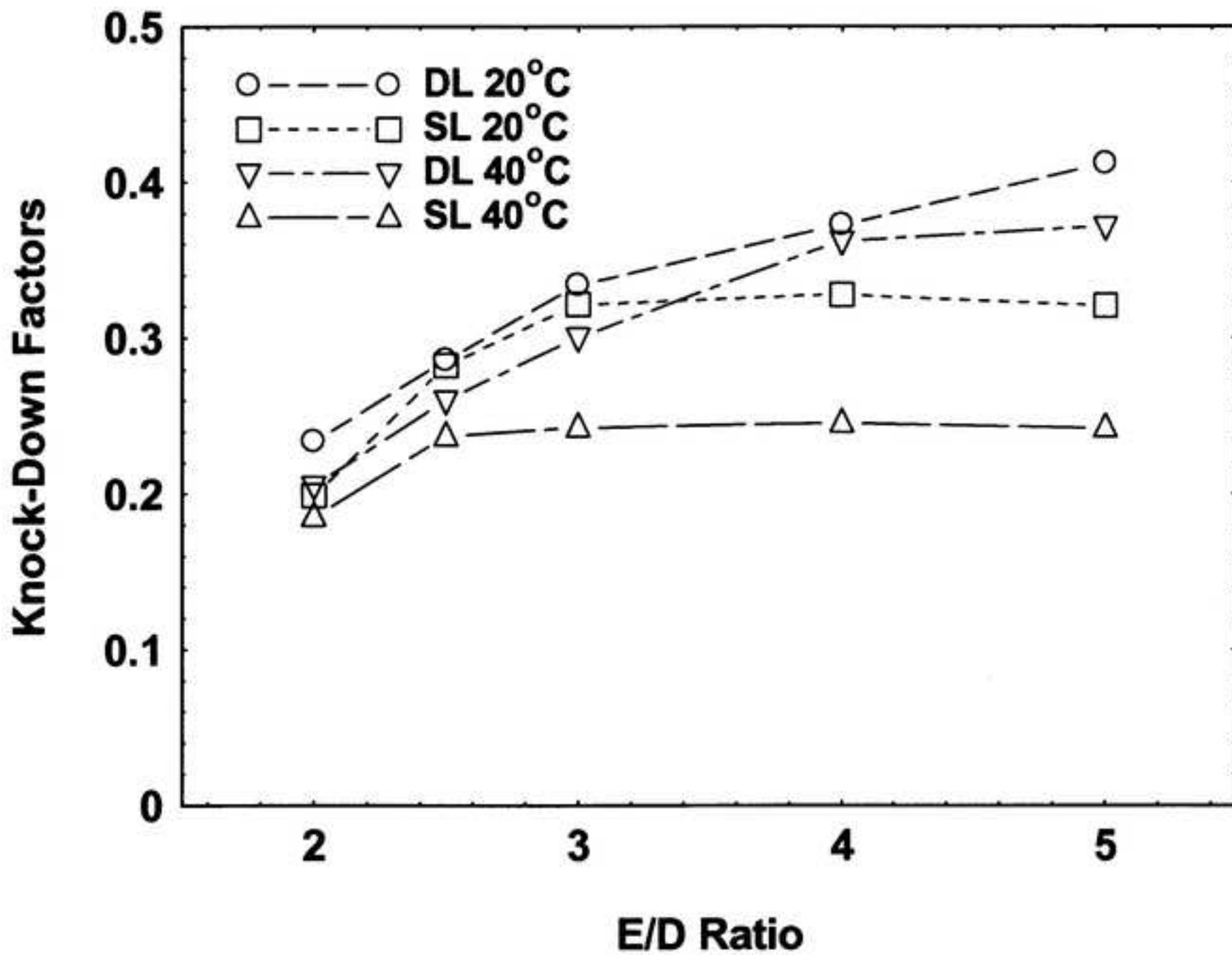












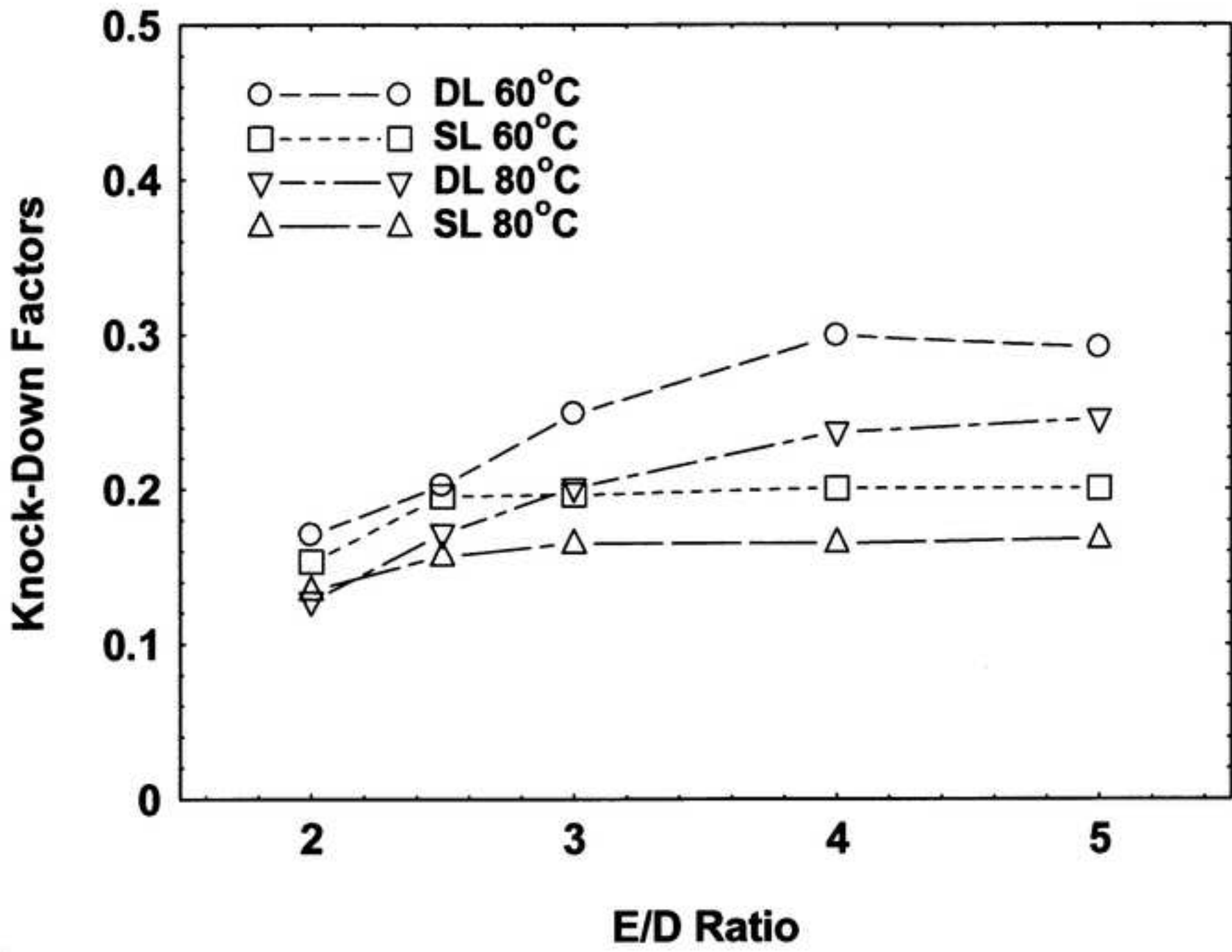


Table 1 rev 1.docx

Table 1

Tensile ultimate loads and stresses of the virgin pultruded GFRP 500 series plate

Coupon	Mean Thickness [mm]	Mean Width [mm]	Mean Cross-Sectional Area [mm ²]	Ultimate Loads [kN]	Ultimate Stress [N/mm ²]	Mean Ultimate Load [kN]	Mean Ultimate Stress [N/mm ²]
1	6.38	25.50	162.7	47.2	290.1	48.2 (0.60)*	300.0 (4.64)*
2	6.39	24.97	159.6	47.8	299.5		
3	6.39	25.00	159.8	48.1	301.0		
4	6.39	25.00	159.8	48.6	304.1		
5	6.38	25.03	159.7	48.3	302.4		
6	6.41	25.30	162.2	49.1	302.7		

*Standard deviation

Table 2(a) rev1.docx

Table 2(a)

Tensile longitudinal elastic moduli of the virgin pultruded GFRP 500 series plate

Coupon	Mean Thickness [mm]	Mean Width [mm]	Mean Cross-Sectional Area [mm²]	Longitudinal Elastic Modulus [MPa]	Mean Longitudinal Elastic Modulus [MPa]
1	6.38	24.83	158.4	24.22	23.13 (2.047)*
2	6.40	25.30	161.9	19.07	
3	6.40	24.27	155.3	24.60	
4	6.39	25.13	160.6	23.78	
5	6.39	25.10	160.4	23.97	

*Standard deviation

Table 2(b) rev1.docx

Table 2(b)

Tensile ultimate loads, stresses, longitudinal elastic moduli and ultimate extensions of the virgin pultruded GFRP 525 series plate

Coupon	Mean Thickness [mm]	Mean Width [mm]	Mean Cross-Sectional Area [mm ²]	Ultimate Loads [kN]	Ultimate Stress [MPa]	Longitudinal Elastic Modulus [GPa]	Ultimate Extension [mm]
1	6.41	39.73	254.7	77.33	303.6	22.74	4.93
2	6.39	39.97	255.4	78.85	308.6	21.59	5.48
3	6.39	39.80	254.3	78.10	307.3	21.63	5.42
4	6.40	39.93	255.6	85.50	334.7	24.34	5.20
Mean Values				79.95 (3.252)*	313.6 (12.35)*	22.58 (1.119)*	5.26 (0.216)*

*Standard deviation

Table 3 rev1.docx

Table 3

Test matrix for pultruded GFRP single-bolt single-lap tension joints [D = 10 mm]

Width to Diameter Ratio [W/D]	Test Temperatures [°C]	End Distance to Hole Diameter Ratio [E/D]	Number of [E/D, °C] Parameter Groups	Number of Nominally Identical Joints per Parameter Group	Total Number of Joints
4	20, 40, 60, 80	2, 2.5, 3, 4, 5	20	6	120

Table 4 rev1.docx

Table 4

Mean ultimate loads and extensions for the range of test temperatures and end distance to bolt/hole diameter ratios of the pultruded GFRP single-bolt single-lap tension joints [D = 10 mm, W/D = 4]

Test Temperature [°C]	End Distance to Bolt/Hole Diameter Ratio [E/D]	Mean Cross-Sectional Area and (Standard Deviation) [mm ²]	Mean Ultimate Load and (Standard Deviation) [kN]	Mean Ultimate Extension and (Standard Deviation) [mm]
20	2	258.1 (2.243)*	15.39 (0.271)*	2.968 (0.112)*
	2.5	257.3 (1.624)	21.82 (0.419)	4.420 (0.228)
	3	255.0 (1.964)*	24.61 (0.870)*	6.120 (0.471)*
	4	256.6 (2.081)*	25.21 (0.579)*	5.954 (0.434)*
	5	255.0 (1.647)	24.52 (1.023)	5.840 (0.534)
40	2	256.3 (1.395)	14.25 (0.612)	3.538 (0.136)
	2.5	256.1 (2.700)*	18.22 (0.640)*	5.446 (0.979)*
	3	256.5 (1.953)*	18.70 (0.461)*	5.400 (0.297)*
	4	258.8 (1.248)	19.05 (0.543)	5.518 (0.154)
	5	257.4 (0.734)*	18.72 (0.290)*	5.072 (0.243)*
60 ¹	2	257.8 (2.242)	11.84 (0.468)	4.045 (0.315)
	2.5	257.4 (1.476)*	15.10 (0.663)*	5.496 (0.680)*
	3	255.1 (1.249)	15.04 (0.627)	6.543 (1.007)
	4	256.5 (3.079)*	15.43 (0.398)*	7.726 (1.304)*
	5	257.8 (1.908)*	15.52 (0.443)*	8.436 (0.847)*
80 ²	2	257.6 (1.836)	10.40 (0.682)	4.277 (0.313)
	2.5	257.0 (1.162)*	12.10 (0.779)*	6.464 (0.720)*
	3	258.9 (2.175)	12.81 (0.858)	8.010 (0.894)
	4	257.6 (1.123)	12.76 (0.397)	8.735 (0.736)
	5	254.7 (2.611)	12.82 (0.320)	8.227 (0.856)

Notes: ¹The joints with E/D = 3 tested at this temperature had EXTREN[®] 525 laps

²All of the joints tested at this temperature had EXTREN[®] 525 laps

*Only five joints in this parameter group gave valid test results

Table 5 rev1.docx

Table 5

Joint failure modes for single-bolt single-lap tension joints [D = 10 mm, W/D = 4]

Test Temperature [°C]	E/D = 2	E/D = 2.5	E/D = 3	E/D = 4	E/D = 5
20	C1 C2 C3 C4 C5 C6	C1 C2 C3 C4 C5 C6	C1 C2 C3 C4 C5 T6	T1 T2 T3 T4 T5 T6	T1 T2 T3 T4 T5 T6
40	C1 C2 C3 C4 C5 C6	C1 C2 C3 C4 C5 C6	T1 T2 T3 C4 T5 C6	T1 T2 T3 T4 T5 T6	T1 T2 T3 T4 T5 T6
60	S1 S2 C3 C4 S5 S6	S1 S2 S3 S4 C5 S6	B1 T2 C3 C4 T5 C6	T1 T2 B3 B4 C5 B6	B1 B2 B3 B4 T5 B6
80	S1 C2 C3 C4 S5 S6	B1 B2 S3 S4 C5 S6	B1 B2 B3 B4 B5 C6	B1 B2 B3 B4 B5 B6	B1 B2 B3 B4 B5 B6

Notes: 1. The letters B, C, S and T denote Bearing, Cleavage, Shear and Tension dominant failure modes, respectively.

2. The numerals 1, 2 etc denote the joint number of the particular [E/D, °C] parameter group.

Table 6 rev1.docx

Table 6

Characteristic mean stresses for the 20 (E/D, °C) parameter groups of single-bolt single-lap tension joints [D = 10 mm, W/D = 4]

Temperature [°C]	Characteristic Mean Stress [N/mm ²]				
	E/D = 2	E/D = 2.5	E/D = 3	E/D = 4	E/D = 5
20	57.90	81.88	90.83	93.38	89.02
40	51.44	66.33	69.92	70.00	70.92
60	42.84	54.05	54.71	56.55	57.76
80	35.62	41.78	43.87	46.65	47.94

Table 7 rev1.docx

Table 7

Characteristic mean overall strains for the 20 (E/D, °C) parameter groups of single-bolt single-lap tension joints
[D = 10 mm, W/D = 4]

Temperature [°C]	Characteristic Mean Overall Strain				
	E/D = 2	E/D = 2.5	E/D = 3	E/D = 4	E/D = 5
20	0.013836	0.020086	0.026359	0.025867	0.024470
40	0.016492	0.018416	0.024326	0.026227	0.023174
60	0.017437	0.021363	0.023807	0.026893	0.034559
80	0.018610	0.025838	0.032140	0.037164	0.033557

Table 8 rev1.docx

Table 8

Mean ultimate stress knock-down factors for single-bolt single-lap tension joints [D = 10 mm, W/D = 4]

Temperature [°C]	Mean Ultimate Stress Knock-Down Factors				
	E/D = 2	E/D = 2.5	E/D = 3	E/D = 4	E/D = 5
20	0.198722	0.282664	0.321702	0.327536	0.320569
40	0.185287	0.237159	0.242993	0.245427	0.24236
60	0.15315	0.195455	0.196488	0.200589	0.200689
80	0.134581	0.156984	0.164951	0.165185	0.167752

Table 9 rev1.docx

Table 9

Characteristic mean ultimate stress knock-down factors for single-bolt single-lap tension joints [D = 10 mm,
W/D = 4]

Temperature [°C]	Characteristic Mean Ultimate Stress Knock-Down Factors				
	E/D = 2	E/D = 2.5	E/D = 3	E/D = 4	E/D = 5
20	0.198454	0.280645	0.311322	0.320062	0.305118
40	0.176312	0.227348	0.239652	0.239927	0.243080
60	0.146835	0.185258	0.187520	0.193826	0.197974
80	0.122088	0.143202	0.150365	0.159894	0.164315

List of Tables & Titles.docx

List of Tables & Titles

Table 1: Tensile ultimate loads and stresses of the virgin pultruded GFRP 500 series plate

Table 2(a): Tensile longitudinal elastic moduli of the virgin pultruded GFRP 500 series plate

Table 2(b): Tensile ultimate loads, stresses, longitudinal elastic moduli and ultimate extensions of the virgin pultruded GFRP 525 series plate

Table 3: Test matrix for pultruded GFRP single-bolt single-lap tension joints [D = 10 mm]

Table 4: Mean ultimate loads and extensions for the range of test temperatures and end distance to bolt/hole diameter ratios of the pultruded GFRP single-bolt single-lap tension joints [D = 10 mm, W/D = 4]

Table 5: Joint failure modes for single-bolt single-lap tension joints [D = 10 mm, W/D = 4]

Table 6: Characteristic mean stresses for the 20 (E/D, °C) parameter groups of single-bolt single-lap tension joints [D = 10 mm, W/D = 4]

Table 7: Characteristic mean overall strains for the 20 (E/D, °C) parameter groups of single-bolt single-lap tension joints [D = 10 mm, W/D = 4]

Table 8: Mean ultimate stress knock-down factors for single-bolt single-lap tension joints [D = 10 mm, W/D = 4]

Table 9: Characteristic mean ultimate stress knock-down factors for single-bolt single-lap tension joints [D = 10 mm, W/D = 4]

List of Figures & Captions

Figure 1(a): Side elevation of a single-bolt single-lap joint subjected to axial tension [Not to scale]

Figure 1(b): Single-bolt single-lap joint just after being clamped by the test machine's grips prior to loading in tension – the packing ensures that the joint's laps are initially straight

Figure 2: Geometry of a GFRP lap of a single-bolt single-lap tension joint subjected to axial tension

Figure 3: (a) Overall view of the elevated temperature test setup, (b) view inside the temperature cabinet showing a tension coupon setup in the mechanical grips and one of the top and bottom insulated semi-circular annuli in place and (c) a view of a single-bolt single-lap joint setup for testing in tension

Figure 4: Typical failure modes: (a) bearing (**B3** [E/D = 4, 80 °C]), (b) cleavage (**C1** [E/D = 2.5, 40 °C]), (c) shear (**S1** [E/D = 2, 60 °C]) and (d) tension (**T2** [E/D = 4, 20 °C])

Figure 5: Mean ultimate stress versus E/D ratio as a function of temperature for single-bolt single-lap joints tested to failure in uniaxial tension [D = 10 mm, W/D = 4]

Figure 6: Mean ultimate stress versus temperature as a function of the E/D ratio for single-bolt single-lap joints tested to failure in uniaxial tension [D = 10 mm, W/D = 4]

Figure 7: Mean ultimate strain versus E/D ratio as a function of temperature for single-bolt single-lap joints tested to failure in uniaxial tension [D = 10 mm, W/D = 4]

Figure 8: Mean ultimate strain versus temperature as a function of the E/D ratio for single-bolt single-lap joints tested to failure in uniaxial tension [D = 10 mm, W/D = 4]

Figure 9: Comparison of mean ultimate stress knock-down factors versus E/D ratio as functions of temperature for single-bolt single- and double-lap tension joints: (a) 20 and 40 °C and (b) 60 and 80 °C test temperatures [Note: DL and SL denote double- and single-lap, respectively]